

# Nuclear and cytoplasmic effects of human CRM1 on HIV-1 production in rat cells

Mika Nagai-Fukataki<sup>1</sup>, Takashi Ohashi<sup>1</sup>, Iwao Hashimoto<sup>2</sup>, Tominori Kimura<sup>3</sup>, Yoshiyuki Hakata<sup>1a</sup> and Hisatoshi Shida<sup>1\*</sup>

<sup>1</sup>Institute for Genetic Medicine, Hokkaido University, Kita-ku, Sapporo 060-0815, Japan

<sup>2</sup>Department of Microbiology, Kansai Medical University, Moriguchi, Osaka 570-8506, Japan

<sup>3</sup>Laboratory of Microbiology and Cell Biology, College of Pharmaceutical Sciences, Ritsumeikan University, Kusatsu, Shiga 525-8577, Japan

The human immunodeficiency virus type 1 (HIV-1) regulatory protein, Rev, mediates the nuclear export of unspliced *gag* and singly spliced *env* mRNAs by bridging viral RNA and the export receptor, CRM1. Recently, rat CRM1 was found to be less efficient than human CRM1 in supporting Rev function in rats. In this study, to understand the role of CRM1 in HIV propagation, the mechanism underlying the function of human and rat CRM1 in HIV-1 replication was investigated in rat cells. The production of viral particles, represented by the p24 Gag protein, was greatly enhanced by hCRM1 expression in rat cells; however, this effect was not simply because of the enhanced export of *gag* mRNA. The translation initiation rate of *gag* mRNA was not increased, nor was the Gag protein stabilized in the presence of hCRM1. However, the processing of the p55 Gag precursor and the release of viral particles were facilitated. These results indicated that hCRM1 exports *gag* mRNA to the cytoplasm, not only more efficiently than rCRM1 but also correctly, leading to efficient processing of Gag proteins and particle formation.

## Introduction

Appropriate animal models for viral infection allow the analysis of viral pathogenesis and oncogenesis, which in turn assist the development of therapeutic and preventative measures. Current animal models of HIV-1 (human immunodeficiency virus-1) disease have used nonhuman primates (Giuffre *et al.* 2003; Hazuda *et al.* 2004; Hu 2005; Veazey *et al.* 2005) and severe combined immunodeficiency mice with transplanted fetal human tissues (Shultz *et al.* 2007; Watanabe *et al.* 2007). These models have made significant contributions to our understanding of lentiviral pathogenesis and have assisted in the development of therapeutic strategies. However, these models have significant shortcomings, such as the limited availability and high

cost of nonhuman primates, the absence of or delay in disease progression, permissivity only for related retroviruses and insufficient viral propagation. For these reasons, new animal models are needed. If viral infection is possible, it would be convenient to use small animal models, in particular mice and rats, as their inbred strains are well characterized and can be genetically manipulated.

Studies on rodent cell-specific defects in the HIV-1 life cycle have facilitated the identification and characterization of the host cell gene products that are essential for viral replication, and these may provide a molecular basis for generating a fully permissive small-animal model. It has been suggested that the major block to HIV-1 replication is at the level of entry and that this hurdle could be overcome by introducing human CD4 and CCR5, which serve as receptors for HIV-1 (Keppeler *et al.* 2001, 2002). Transgenic (Tg) rats, expressing human CD4 and CCR5, have been reported to support some replication of HIV-1, albeit very poorly (Keppeler *et al.* 2002; Goffinet *et al.* 2007). In contrast, Tg mice

Communicated by: Haruhiko Siomi

\*Correspondence: hshida@igm.hokudai.ac.jp

<sup>a</sup>Present address: Department of Immunology, Kinki University School of Medicine, 377-2 Ohno-Higashi, Osaka-sayama, Osaka 589-8511, Japan.

DOI: 10.1111/j.1365-2443.2010.01476.x

© 2010 The Authors

Journal compilation © 2010 by the Molecular Biology Society of Japan/Blackwell Publishing Ltd.

Genes to Cells (2010) 1

expressing human CD4/CCR5 do not allow the propagation of HIV-1 (Browning *et al.* 1997). These results support the rat as a promising small-animal model candidate.

Analyses have showed novel interactions between rodent and viral factors. A notable example is CRM1 (chromosome region maintenance 1; exportin 1), a member of the karyopherin family of nucleocytoplasmic-transport factors (Neville *et al.* 1997; Cullen 2003) that is involved in nuclear export. In the nucleus, CRM1 binds its cargo in the presence of a GTP-bound form of the Ran GTPase (RanGTP), and following nuclear export, hydrolysis of GTP to GDP causes a conformational shift that induces cytoplasmic cargo release, providing directionality for this export pathway (Fornerod *et al.* 1997; Neville *et al.* 1997; Nakielny & Dreyfuss 1999; Cullen 2003). Human CRM1 cooperates with HIV-1 Rev and the human T cell leukemia virus type 1 (HTLV-1) Rex proteins to transport 4 kb of partially spliced and 9 kb of unspliced mRNAs encoding viral structural proteins and genomes (Cullen 1998). Rev or Rex multimerizes on viral RNA to recruit several CRM1 molecules; furthermore, the recruitment of CRM1 enhances Rev or Rex interactions vice versa (Hakata *et al.* 2002). Rat CRM1, which exhibits 98% amino acid identity to its human counterpart, is able to bind efficiently to Rex, but cannot induce the multimerization of Rex proteins on its cognate RNA. This results in the breakdown of HTLV-1 RNA transport in rat cells (Hakata *et al.* 2001). Thus, rat CRM1 represents a major factor in the human–rat species barrier to HTLV-1 (Zhang *et al.* 2006; Takayanagi *et al.* 2007). Furthermore, detailed comparisons of human and rat CRM1 proteins identified the domains essential for the induction of Rex multimerization and the binding of RanBP3, another component involved in RNA export (Hakata *et al.* 2003). These analyses suggested that CRM1 functions not only in RNA export out of the nucleus but also in the formation of the transport complex that includes viral RNA and various cellular components (Hakata *et al.* 2003).

In contrast to the definitive results obtained for rat CRM1–Rex interactions, the existence of a profound block in Rev function in rodent cells remains controversial, although a reduced level of the 9-kb transcript has been generally reported (Bieniasz & Cullen 2000; Keppler *et al.* 2001). Some studies have found impaired Rev activity (Marques *et al.* 2003), whereas others have ascribed the reduced transcript level to oversplicing or to the reduced stability of unspliced transcripts in rodent cells compared to human cells

(Malim *et al.* 1991), a problem that is corrected by the expression of the human p32 protein (Zheng *et al.* 2003). These contradictory results seem to stem partly from the use of different cells and reporters for evaluating Rev activity and partly from the limited investigation of cellular cofactors. However, recently, we found that Gag production was increased by hCRM1 in rat macrophages in contrast to its marginal effect in rat T cells (Okada *et al.* 2009).

In this study, we have compared the molecular mechanisms underlying the function of human and rat CRM1 proteins in HIV propagation in rat cells. We show that the expression of hCRM1 in rat cells not only enhances the export of HIV *gag* mRNA but also restores the processing of the precursor Gag protein and release of viral particles, leading to efficient virus production.

## Results

### Enhanced p24 production in hCRM1-transfected rat cells

Recently, we found that hCRM1 enhanced Gag production in rat macrophages (Okada *et al.* 2009); therefore, it was decided to examine the molecular mechanism involved in this process using convenient rat cell lines. ER1/neo1 cells are particularly useful because they, like rat macrophages, support the efficient expression of HIV-1 genes without the need for human cyclin T1 (unpublished results [Okada *et al.* 2009;]). The initial step involved transfecting the hCRM1-expressing plasmid into ER1/neo1 cells along with the reporter pCRRE (Kimura *et al.* 1996), which harbors the HIV-1 genome, including the intact *gag* and *rev* sequences (Fig. 1A). Next, the production of the Gag protein, p24, in the medium was measured by ELISA. In addition, cells were simultaneously cotransfected with pCDM $\beta$ -gal, which was used to normalize the transfection efficiency, and pH1-luc, which acted as a surrogate marker for total gene expression driven by the HIV-1 LTR. In comparison with untransfected rat cells, hCRM1-transfected cells produced increasing levels of p24 in the culture supernatant with increasing amounts of pSR $\alpha$ hCRM1. On the other hand,  $\beta$ -gal and luc activities remained at similar levels in both hCRM1-transfected and untransfected rat cells, indicating similar transfection efficiencies and HIV LTR-mediated transcription, irrespective of hCRM1 expression (Fig. 1B). These results showed the enhancement of p24 production after transfection with hCRM1.

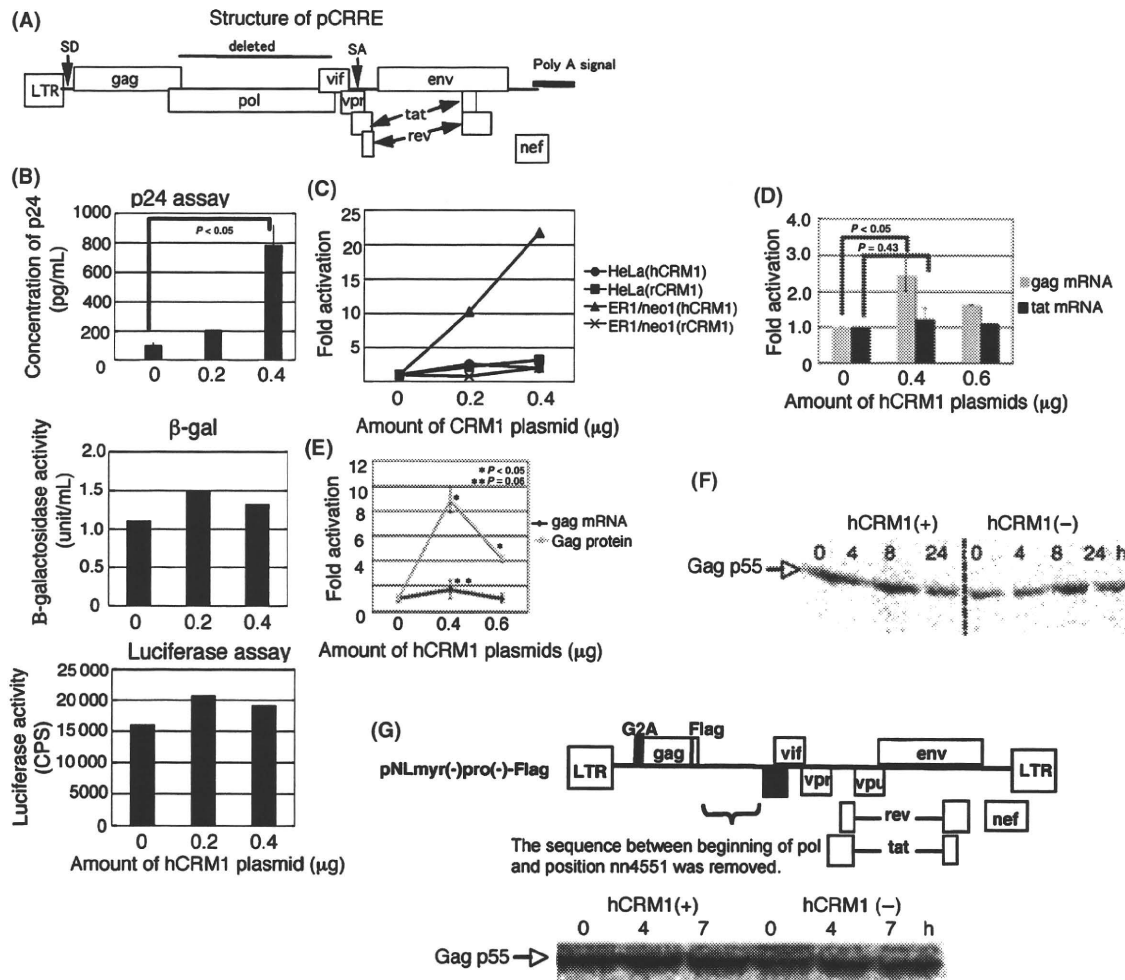


**Figure 1** Effect of CRM1 on p24 production. (A) The structure of pCRRE. (B) ER1/neo1 cells ( $1 \times 10^5$ ) were transfected with 1.6  $\mu$ g of pCRRE and pSR $\alpha$ hCRM1 as indicated, 0.1  $\mu$ g of pCDM $\beta$ -gal, and 0.3  $\mu$ g of pH1-luc using TransIT-LT1 (Mirus) reagent. The total abundance of transfected plasmids was adjusted with pSR $\alpha$ 296. Two days after transfection, p24 was quantified from the cell culture medium using a RETRO-TEK HIV-1 p24 Antigen ELISA kit (ZeptoMetrix). Cytoplasmic  $\beta$ -gal activity was measured using standard colorimetric methods ( $\beta$ -gal assay) (Hakata *et al.* 2001), and luciferase activities were also quantified. (C) ER1/neo1 and HeLa cells were transfected with pCRRE, pCDM $\beta$ -gal and pH1-luc along with pSR $\alpha$ hCRM1 or pSR $\alpha$ rCRM1 as described earlier. The amount of p24 in the medium was quantified as in (B). The value of the control sample without CRM1 was set at 1. The  $\beta$ -galactosidase and luciferase activities were similar in all samples (data not shown). These data are representative of three independent experiments. (D) The amount of mRNA in cytoplasmic fraction in ER1/neo1 cells was indicated. ER1/neo1 cells were transfected with pCRRE, pSR $\alpha$ hCRM1, pCDM $\beta$ -gal and pH1-luc and then separated into nuclear and cytoplasmic fractions using an NP40 detergent-containing buffer, as described in Materials and Methods. Quantitative RT-PCR was used to determine the abundance of *gag*, *tat* and  $\beta$ -gal mRNAs in each fraction. The ratios of *gag* mRNA/ $\beta$ -gal mRNA and *tat* mRNA/ $\beta$ -gal mRNA were calculated. The value of the control sample without hCRM1 was set at 1. These values are the means of three independent sets of experiments, and the SD was calculated. (E) Gag protein (p24) in the medium and  $\beta$ -gal activity were quantified, and the Gag/ $\beta$ -gal ratio was plotted and compared to the ratio of cytoplasmic *gag* mRNA/ $\beta$ -gal mRNA. These data are representative of three independent experiments. (F) Stability of Gag protein in rat cells. At 48 h post-transfection, cells were pulse-labeled with [ $^{35}$ S]-methionine/cysteine and chased for 0, 4, 8 and 24 h. The medium and cells were solubilized with detergent-containing buffer and combined. Then, Gag proteins were immunoprecipitated using anti-Gag antibodies and protein-G Sepharose and analyzed by SDS-PAGE followed by autoradiography. (G) ER1/neo1 cells were transfected with pNLmyr(-)pro(-)Flag, pSR $\alpha$ hCRM1 and pCDM $\beta$ -gal. At 40 h post-transfection, cells were pulse-labeled with [ $^{35}$ S]-methionine/cysteine and chased for 0, 4 and 7 h. Gag proteins in the cell lysates were immunoprecipitated using anti-FLAG antibodies and protein-G Sepharose.

Next, we compared the effect of hCRM1 and rCRM1 in HeLa and ER1/neo1 cells by measuring p24 production. After transfection of either of the CRM1-expressing plasmids into HeLa cells, a small enhancement of p24 production was observed, although the differences between rat and human CRM1 were not significant (Fig. 1C). In addition, the same results were obtained in other human cell lines, including 293T and HOS cells (data not shown). In contrast, p24 production increased markedly in ER1/neo1 cells after transfection with the hCRM1-expressing plasmid, whereas expression of rCRM1 had no detectable effect (Fig. 1C). As expected, no significant changes in  $\beta$ -gal or luc activities were observed after transfection with human and rat CRM1-expressing plasmids (data not shown). In addition, hCRM1 enhanced expression of Gag in other rat cell lines (REF52, W31, FPM-SV and NR8383 cells [Okada *et al.* 2009]), whereas rCRM1 did not (data not shown). These results suggested that rCRM1 is a poor cofactor for Rev.

#### Effect of hCRM1 on the export of *gag* mRNA

The aforementioned results indicated that hCRM1 enhanced p24 production in rat cells; thus, the next step was to examine the mechanism underlying this phenomenon. It is conceivable that hCRM1 may export *gag* mRNA more efficiently than rCRM1. To investigate this possibility, hCRM1- or mock-transfected cells were separated into their nuclear and cytoplasmic fractions, and *gag* mRNA levels in the cytoplasmic fractions were compared using quantitative RT-PCR. To confirm augmented levels of Gag protein in these hCRM1-transfected cells, the medium was collected and subjected to a p24 ELISA. In the cytoplasm of hCRM1-transfected rat cells, the increase in *gag* mRNA levels was two to three times that of the mock-transfectants. A similar increase in *gag* mRNA was also observed in the nuclear fraction in the presence of hCRM1 (data not shown). On the other hand, hCRM1 expression had no effect on *tat* mRNA levels, because CRM1 is not involved in that particular export pathway (Fig. 1D). No signals were detected in the samples that had not been subjected to a reverse transcriptase (RT) reaction (data not shown). Efficient separation of the cytosolic and nuclear fractions was confirmed by amplification of  $\beta$ -actin pre-mRNA, which was detected exclusively in the nuclear fraction (data not shown). In contrast to the small increase in *gag* mRNA levels in the cytoplasm, at its peak, the production of p24 from

hCRM1-transfected rat cells was nine times greater than in the mock-transfectants (Fig. 1E). p24 Gag production and the efficiency of *gag* mRNA export was decreased by transfection of 0.6  $\mu$ g hCRM1 expression plasmids (Fig. 1D,E). Too much hCRM1 may affect nuclear export adversely because of imbalance with other factors. These results showed that hCRM1 modestly enhanced *gag* mRNA export in rat cells but greatly increased Gag protein production, suggesting that hCRM1 may function in the cytoplasm.

#### Stability of Gag protein

Next, we examined whether hCRM1 has an effect on Gag protein stability. A [<sup>35</sup>S]-methionine/cysteine pulse-chase analysis of the Gag protein was carried out in rat cells transfected with pCRRE. An inhibitor against HIV-1 protease was added to prevent processing of the Gag precursor, which would hamper the assessment of Gag stability. As Gag proteins are released as viral particles into the medium, the total amount of Gag protein in both the cell and the medium should be quantified to assess its stability. Thus, the total cell culture including both cell lysates and medium was dissolved with the detergent solution and then immunoprecipitated with an anti-p24 monoclonal antibody (mAb), followed by SDS-PAGE and autoradiography. The Gag protein was highly stable, irrespective of the presence or absence of hCRM1 (Fig. 1F). The stability of the Gag protein was ascertained using another plasmid, pNL-myr(-)pro(-)Flag, which exclusively expresses intracellular, nonmyristoylated p55 Gag because of a G2A mutation at the 5' region of the *gag* gene (Kawada *et al.* 2008) (Fig. 1G). These results excluded the involvement of hCRM1 in Gag protein stability.

The small increase in intensity of p55 Gag bands in the presence of hCRM1 (Fig. 1F,G) corresponded to the enhancement of *gag* mRNA in the cytoplasm (Fig. 1D,E), suggesting that the efficiency of *gag* mRNA translation was not elevated by hCRM1 expression. It is consistent with the results of polyribosome analysis that indicated a constant rate of translation initiation irrespective of hCRM1 expression (Data S1, Fig. S1 in supporting information).

#### Effect of hCRM1 on the export of *gag* mRNA and p24 production using pCMV $\Delta$ R8.2

Next, the effect of hCRM1 was examined further using the plasmid, pCMV $\Delta$ R8.2, which generates



higher levels of Gag protein in the medium of ER1/neo1 cells, compared to other reporters, such as pCRRE. The results showed that pCMV $\Delta$ R8.2 synthesized Gag at 20- to 30-fold higher levels in the presence of hCRM1 than in its absence (Fig. 2A). As with the other reporters, a slight increase in cytoplasmic *gag* mRNA levels was observed in the presence of hCRM1 (Fig. 2B), whereas *tat* and  $\beta$ -*gal* mRNA levels were not affected (Fig. 2C,D). A similar increase in *gag* mRNA was also observed in the nuclear fraction in the presence of hCRM1 (data not shown). Efficient separation of the cytosolic and nuclear fractions was confirmed by the amplification of  $\beta$ -*actin* pre-mRNA, which was detected exclusively in the nuclear fraction (Fig. 2E), and  $\beta$ -galactosidase (as a cytoplasmic marker), of which approximately 95% was detected in the cytoplasmic fraction (Fig. 2F).

### FISH analysis of *gag* mRNA

As part of our further investigation into the effect of hCRM1 on the export of *gag* mRNA in rat cells, the

intracellular distribution of *gag* mRNA was analyzed using a fluorescence *in situ* hybridization assay (FISH). As this method does not require the physical separation of the cytoplasmic and the nuclear fractions, it was possible to rule out the leakage of mRNAs from the nuclear fraction during the process. ER1/neo1 cells were cotransfected with pCMV $\Delta$ R8.2 and pSR $\alpha$ hCRM1, pSR $\alpha$ rCRM1 or the pSR $\alpha$ 296 control vector. The intracellular distribution of *gag* mRNA was visualized using a DIG-labeled minus strand DNA probe [nucleotides (nts) 964 to 798 of HIV-1<sub>NL4-3</sub> provirus], which is complementary to the *gag* coding region. The *gag* mRNA was distributed throughout the nucleus and cytoplasm of some cells, but was confined to the nucleus of other cells, irrespective of hCRM1 or rCRM1 expression. Both patterns of *gag* mRNA distribution were observed in HeLa and ER1/hCRM1-7 cells, which constitutively express hCRM1 (Fig. 3A). Control experiments demonstrated that the signals detected were specific for HIV-1 *gag* mRNAs; first, mock-transfected cells exhibited no signal after hybridization with the same probe and second, hybridization with the plus strand

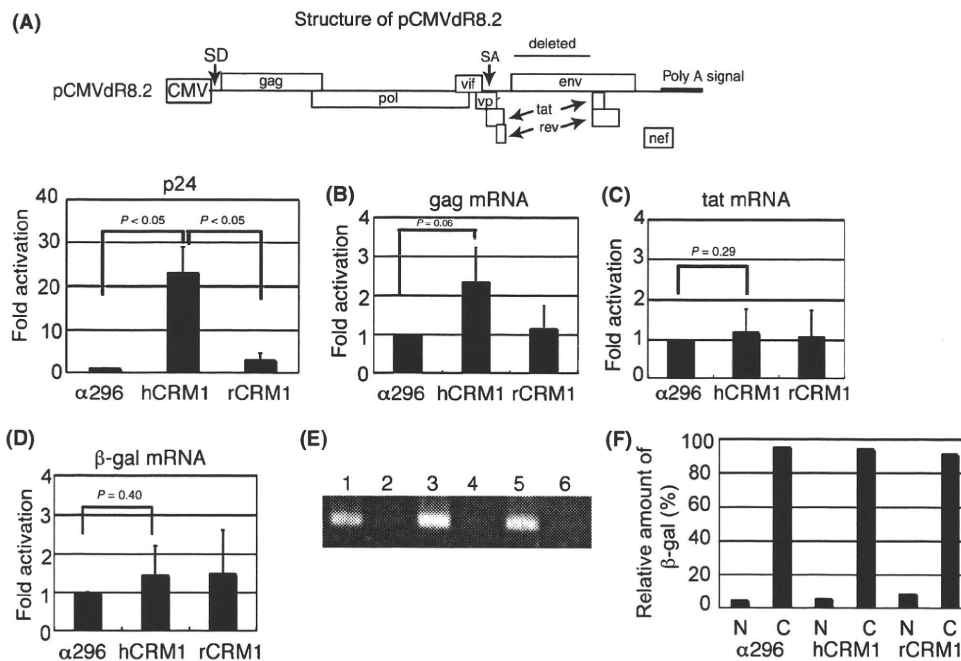


**Figure 2** Effects of rat and human CRM1 on the production of Gag protein and *gag* mRNA derived from pCMV $\Delta$ R8.2 in rat cells. (A–D) ER1/neo1 cells were transfected with pCMV $\Delta$ R8.2 (1.6  $\mu$ g) and pCDM $\beta$ -gal (0.1  $\mu$ g) along with pSR $\alpha$ hCRM1 (0.4  $\mu$ g) or pSR $\alpha$ rCRM1 (0.4  $\mu$ g). The level of p24 in the medium and cytoplasmic  $\beta$ -gal activity, *gag* mRNA, *tat* mRNA and  $\beta$ -gal mRNA were quantified. The average and SD were calculated based on three independent sets of experiments. (E) PCR fragments of  $\beta$ -actin pre-mRNA in the nucleus (lanes 1, 3 and 5) and cytoplasm (lanes 2, 4 and 6) of cells without (lanes 1 and 2) or with (lanes 3 and 4) hCRM1 and (lane 5 and 6) rCRM1. (F)  $\beta$ -gal activity in the nuclear and cytoplasmic fractions was quantified, and the ratios of the  $\beta$ -gal activities in each fraction were calculated.

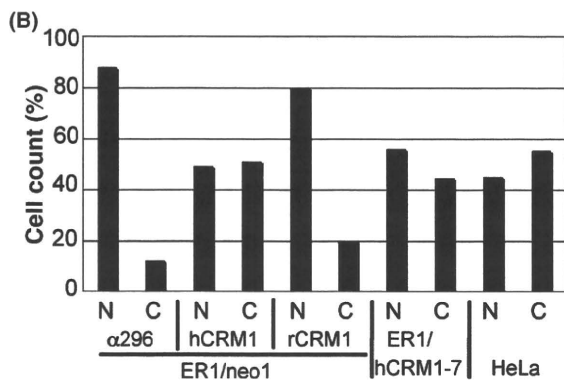
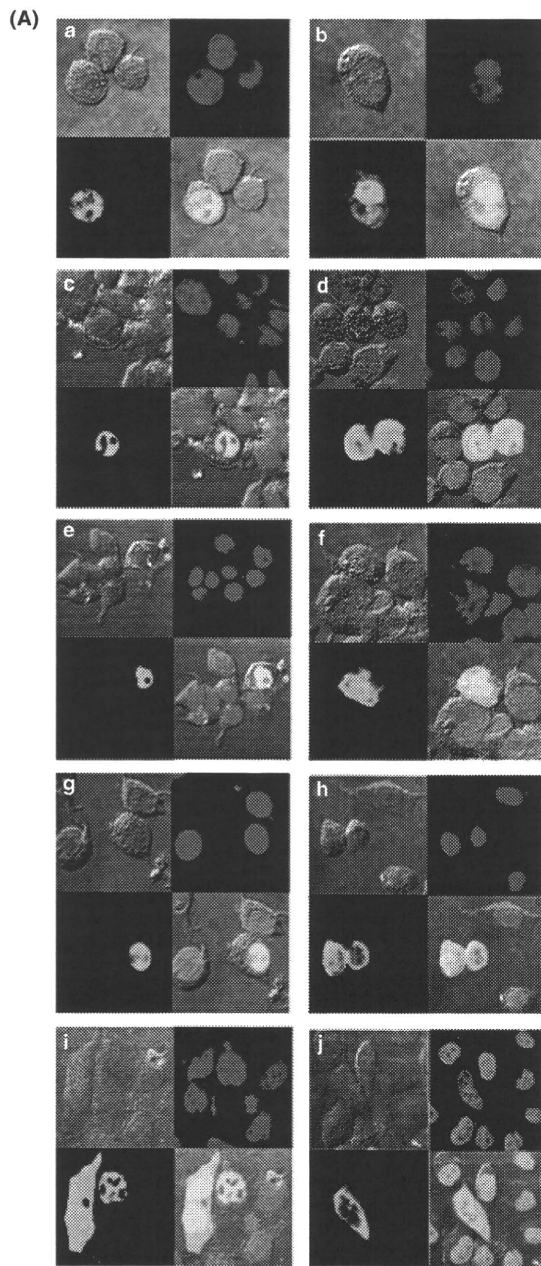


**Figure 3** Fluorescence *in situ* hybridization (FISH) profiles of *gag* mRNA distribution in cells. (A) ER1/neo1 cells (panels a–f) were transfected with pCMVΔR8.2, along with pSRα296 (panels a and b), pSRαhCRM1 (panels c and d) or pSRαrCRM1 (panels e and f). ER1/hCRM1-7 (panels g and h) and HeLa cells (panels i and j) were transfected with pCMVΔR8.2. Cells were subjected to *in situ* hybridization. In all panels, the upper left image is phase contrast and the upper right shows DAPI-stained cells. The lower left image shows the FISH profile and the lower right is a merged image. (B) The number of cells (designated N) in which *gag* mRNA is localized exclusively to the nucleus and those (designated C) which contain *gag* mRNA distributed throughout the cytoplasm and nucleus. More than 150 cells were counted and their ratios are presented. These data represent the total number of cells counted in three independent experiments.

DNA probe (nts 798–964 of the HIV-1<sub>NL4-3</sub> provirus) failed to show any signals in the transfected cells (data not shown). Fig. 3B shows the percentage of cells positive for the nuclear or cytoplasmic accumulation of *gag* mRNA. An approximately threefold increase in the cytoplasmic distribution of *gag* mRNA was observed in cells with constitutive or transient expression of hCRM1. These results were consistent with the quantification of cytoplasmic *gag* mRNA using RT-PCR (see Fig. 2B).

**Effect of hCRM1 on the processing of Gag protein**

We examined the processing of the Gag precursor and the release of viral particles using Western blot analysis. ER1/neo1 cells were transfected with pCMVΔR8.2, pCDMβ-gal and pSRαhCRM1-HA or pSRαrCRM1-HA as described earlier, and cell lysates and virus-like particle (VLP) fractions were prepared from the culture medium (Fig. 4A). The hCRM1 construct enhanced expression of the p55 Gag precursor approximately threefold, whereas it had a remarkable effect on the efficient processing of Gag (increasing it by approximately 10-fold) and on the formation of viral particles. The amount of VLP was evaluated by the p24 ELISA assay because the p24 bands of the VLP fractions, prepared from pSRα296 and pSRαrCRM1-transfected cells, were too faint in the Western blot profile to be quantified. The ELISA showed a 70-fold increase in VLP in response to the expression of hCRM1, whereas rCRM1 had no effect (data not shown). Less hCRM1 protein was expressed than rCRM1 protein (Fig. 4A), and it is possible that the hCRM1-HA protein may be unstable in ER1/neo1 cells, as shown

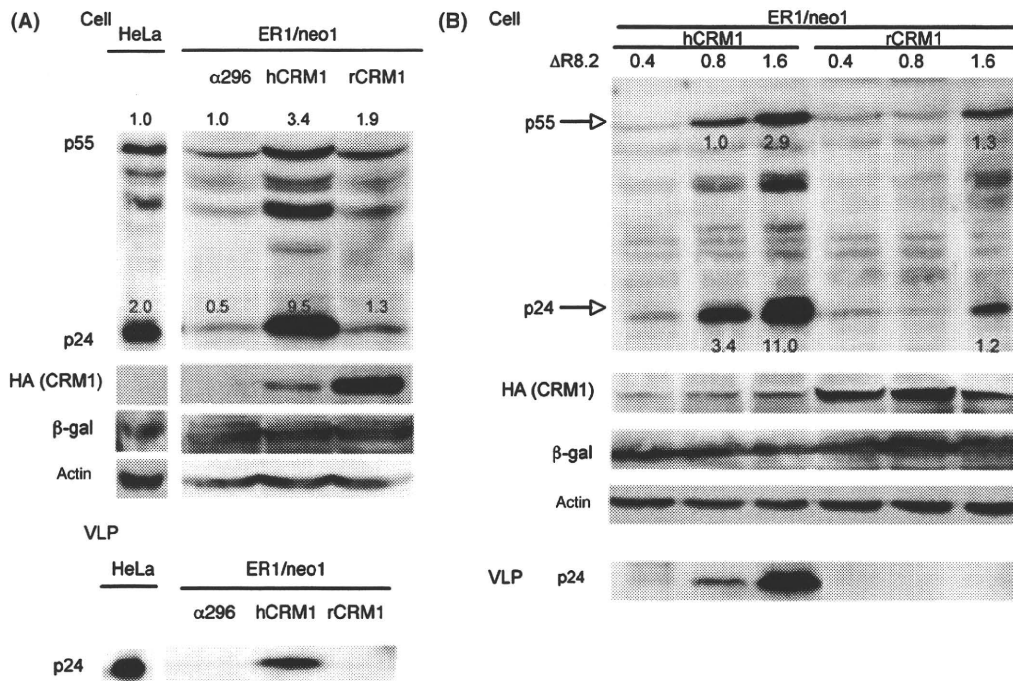


**Figure 4** Western blotting of Gag proteins expressed in ER1/neo1 cells. (A) ER1/neo1 and HeLa cells were transfected with pCMVΔR8.2 and pCDMβ-gal along with the empty vector, pSRα296, and pSRαhCRM1-HA or pSRαrCRM1-HA as described earlier. Fractions corresponding to approximately  $1.5 \times 10^4$  and  $5 \times 10^5$  ER1/neo1 cells were subjected to Western blotting to analyze Gag protein profiles in the cell and VLP fractions, respectively. Fractions corresponding to approximately  $5 \times 10^3$  and  $5 \times 10^4$  HeLa cells were subjected to SDS-PAGE for analysis of the cell and VLP fractions, respectively. The intensities of the Gag proteins were quantified by LAS-1000. The amount of p55 Gag in pSRα296-transfected ER1/neo1 cells was set at 1.0, and the relative amounts of Gag protein were calculated. The ratio of p24/p55 expressed in HeLa was also presented. (B) ER1/neo1 cells were transfected with pCMVΔR8.2 (0.4–1.6 μg) and pCDMβ-gal (0.1 μg) along with pSRαhCRM1-HA (0.4 μg) or pSRαrCRM1 (0.4 μg). Fractions corresponding to approximately  $2 \times 10^4$  and  $5 \times 10^5$  cells were subjected to Western blotting to analyze Gag protein profiles in the cell and VLP fractions, respectively. The intensity of the p55 Gag band in the lane representing ER1/neo1 cells, transfected with 0.8 μg of pCMVΔR8.2 and pSRαhCRM1, was quantified and set at 1.0.

previously (Okada *et al.* 2009). The slight increase in p55 Gag protein in the presence of hCRM1 is consistent with the slight increase in *gag* mRNA observed in the cytoplasm (see Figs 1D,E and 2B). In addition, the remarkable increase in VLP is consistent with the increase in p24 detected by ELISA in the culture supernatant, as described earlier (Figs 1B and 2A). In human HeLa cells, which support high levels of HIV-1 production, both efficient processing and particle release were observed (Fig. 4A).

Next, to investigate whether the amount of Gag protein in the cells affected the processing of Gag and the release of viral particles, cells were transfected with various amounts of pCMVΔR8.2, together with pSRαhCRM1-HA or pSRαrCRM1-HA. The proportions of the p55 and p24 Gag proteins were similar, irrespective of the amount of p55 in the

hCRM1-transfected cells (Fig. 4B). In contrast, the ratio of p24/p55 in the rCRM1-transfected cells was less than in the hCRM1-expressing cells, even when the rCRM1-transfected cells contained more p55. Moreover, the bands of p24 were clearly detected in the VLP fractions that were prepared from hCRM1-transfected cells, but not in the fractions from rCRM1-transfected cells (Fig. 4B). The relative amounts of p24, as quantified by ELISA, were 4.6, 59 and 1 in the VLP fractions of 0.8 μg pCMVΔR8.2/pSRαhCRM1-, 1.6 μg pCMVΔR8.2/pSRαhCRM1- and 0.8 μg pCMVΔR8.2/pSRαrCRM1-transfected cells, respectively (data not shown), consistent with the Western blotting profiles (Fig. 4B). These results suggested that the efficiency of Gag protein processing was enhanced by hCRM1-mediated *gag* gene expression but not by the amount of intracellular Gag protein.

**Effect of hCRM1 on membrane trafficking and the release of p55 Gag**

To examine the effect of hCRM1 on the destination of the Gag protein, in the absence of Gag processing, the p55 Gag protein was expressed using pNLmyr(-)pro(-)Flag and pNLmyr(+)-pro(-)Flag because these vectors express only uncleaved p55, while the FLAG tag supports clear images in immunofluorescent assays. Moreover, the amount of p55 expressed by pNLmyr(-)pro(-)Flag may reflect the amount of

*gag* mRNA in the cytoplasm more accurately because it is not released into the medium because of the lack of myristoylation.

When pNLmyr(-)pro(-)Flag was transfected into ER1/neo1 cells, hCRM1 expression augmented the amount of intracellular p55 by 3.3- or 2.5-fold more than the empty vector or rCRM1 expression, respectively (Fig. 5A). This moderate increase in p55 Gag protein in the presence of hCRM1 reflected the small enhancement of *gag* mRNA observed in the cytoplasm (see Figs 1D,E and 2B), consistent with the

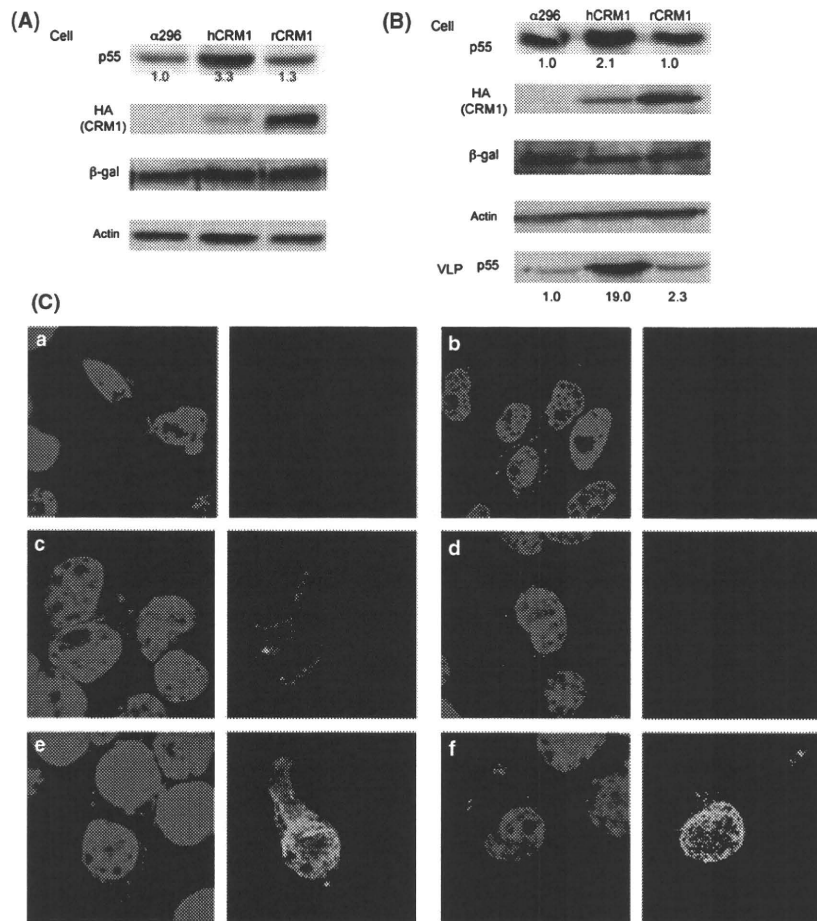


**Figure 5** Effect of hCRM1 on membrane trafficking and release of virus particles using pNLmyr(-)pro(-)Flag and pNLmyr(+)-pro(-)Flag. Approximately,  $2 \times 10^4$  ER1/neo1 cells transfected with pNLmyr(-)pro(-)Flag along with pSR $\alpha 296$ , pSR $\alpha$ hCRM1 or pSR $\alpha$ rCRM1 were subjected to Western blotting (A). The cells and VLP fractions corresponding to approximately  $5 \times 10^3$  and  $5 \times 10^5$  cells transfected with pNLmyr( $\pm$ )pro(-)Flag along with pSR $\alpha 296$ , pSR $\alpha$ hCRM1 or pSR $\alpha$ rCRM1 were subjected to Western blotting, respectively (B). The band intensity of p55 Gag expression in pSR $\alpha 296$ -transfected cells was set at 1.0. (C) HeLa cells were transfected with pNLmyr(-)pro(-)Flag (panel a) or pNLmyr(+)-pro(-)Flag (panel b). ER1/neo1 cells were transfected with pNLmyr(-)pro(-)Flag and pSR $\alpha$ hCRM1 (panel c), or pNLmyr(+)-pro(-)Flag along with pSR $\alpha 296$  (panel d), pSR $\alpha$ hCRM1 (panel e), or pSR $\alpha$ rCRM1 (panel f). Cells were subjected to direct immunofluorescence assay. In all panels, the left image is a merged picture of DAPI (blue) and p55 Gag protein (red), and the right-hand panels show exogenous CRM1 (green).

results described in Fig. 1F,G and S1. When pNL-myr(+)*pro(-)*Flag was transfected into ER1/neo1 cells, hCRM1 expression enhanced the intracellular p55 level by twofold compared to the empty vector or rCRM1 expression. In contrast, hCRM1 expression augmented VLP production by 19- or 8-fold compared to the empty vector or rCRM1 expression, respectively (Fig. 5B). These results suggested that hCRM1 promotes the release of viral particles independent of the processing of p55.

Next, immunofluorescence was used to examine the localization of p55 Gag in the presence or absence of hCRM1. Unmyristoylated p55 was distributed diffusely throughout the cytoplasm of both HeLa and hCRM1-expressing ER1/neo1 cells transfected with pNLmyr(-)Gag-Flag (Fig. 5C panels a and c). On the other hand, myristoylated Gag was characterized by its

punctate state on the plasma membranes of HeLa and ER1/neo1 cells transfected with pNLmyr(+)*Gag-Flag*, irrespective of the expression of human or rat CRM1 (Fig. 5C panels b, d, e and f). The ratio (20–30%) of rat cells that showed the punctate Gag profile was not increased by the expression of hCRM1, whereas almost HeLa cells showed the punctate profiles. These results suggest that the membrane trafficking of p55 Gag occurred in the rat cells inefficiently compared to the human cells and it was not restored by hCRM1.

**Region of hCRM1 responsible for the up-regulation of p24 production**

To identify the region of hCRM1 responsible for the production of p24, we compared the ability of the two chimeric CRM1s to produce p24: hrCRM1 consisted

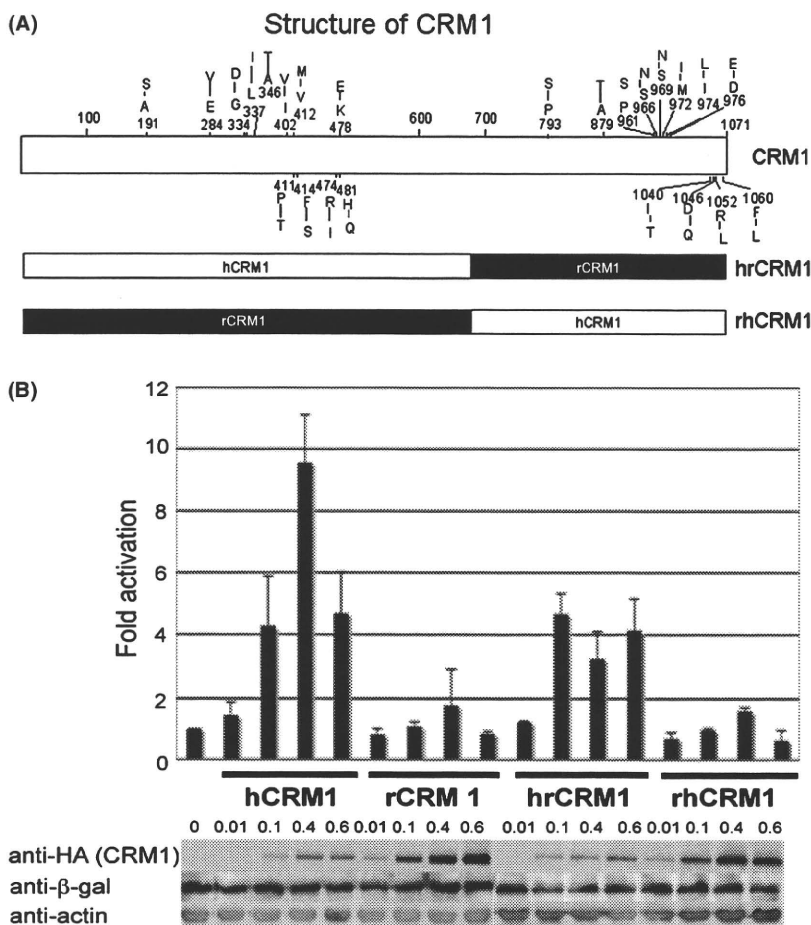


**Figure 6** Analysis of the region of hCRM1 responsible for the up-regulation of p24 production in ER1/neo1 cells. (A) Structure of CRM1. (B) ER1/neo1 cells were transfected with pCMVΔR8.2, pCDMβ-gal and various CRM1-expressing plasmids. HIV-1 p24 in the medium was quantified by ELISA. The protein expression of CRM1, β-gal and actin was analyzed by Western blotting.



of the N-terminal half of hCRM1 [amino acids (aa) 1–679] and the C-terminal half of rCRM1 (amino acids (aa) 680–1072), whereas rhCRM1 was its reverse chimera (Fig. 6A). Expression of hrCRM1-HA increased p24 production, whereas there was little enhancement of p24 production by rhCRM1-HA. It should be noted that hCRM1, when expressed at the same level as rCRM1, augmented p24 production but that rCRM1 had no effect, which ruled out the possibility that over-expression of rCRM1 inhibited p24 production. No significant changes in  $\beta$ -gal activity were observed after transfection with CRM1-expressing plasmids (Fig. 6B). These results indicated that the N-terminal region of hCRM1 was involved in the enhanced production of p24.

## Discussion

Although initial reports suggested that only fully spliced viral transcripts are detectable and that the effects of Rev are diminished in murine cells (Trono & Baltimore 1990), these findings were not reproduced (Malim & Cullen 1991; Bieniasz & Cullen 2000; Keppler *et al.* 2001). Instead, it was proposed that excessive splicing was responsible for a significant reduction in the levels of viral unspliced RNA species and Gag protein in rodent cells (Zheng *et al.* 2003). Moreover, it has been reported that some rat cells exhibit largely unimpaired expression of Env, a Rev-dependent HIV-1 gene product that is translated from a partially spliced viral mRNA (Keppler *et al.* 2001). One reason for these inconsistent conclusions may have been because of lack to examine the cellular cofactors of Rev, such as CRM1. In both our recent studies and the present study, we found that expression of hCRM1, but not rCRM1, enhanced production of the Gag protein in various rat cells, including macrophages (Okada *et al.* 2009), supporting previous findings of poor Rev activity in these cells.

Although significant export of *gag* mRNA into the cytoplasm of rat cells was observed, we found that hCRM1 enhanced *gag* mRNA export two- to three-fold as indicated by quantitative RT-PCR after cell fractionation and *in situ* hybridization. This increase was in sharp contrast to the 10- to 30-fold augmentation of the Gag protein in the medium. This phenomenon is quite interesting as it has been firmly established that CRM1 is an export factor for Rev, which bridges CRM1 and the viral *gag/env* mRNAs (Cullen 1998, 2003). The aforementioned results suggested that, in addition to simple nucleocytoplasmic transport, CRM1 is somehow involved in regulation

of gene expression in the cytoplasm, which affects destination of the cognate protein.

To determine the step during which the activity of hCRM1 differs from that of rCRM1, we examined the stability of the Gag protein using a pulse label and chase experiment. However, the results suggested that hCRM1 does not play a role in prolonging the life of the Gag protein. Neither polyribosome profiling analysis nor the quantification of p55 Gag supported the enhancement of *gag* mRNA translation efficiency by hCRM1. Instead, the data showed that the p55 Gag precursor that was synthesized in the presence of hCRM1, but not rCRM1, underwent efficient processing to the mature Gag protein and budding of virus particles into the culture medium. The results that hCRM1 affects the efficient processing and budding of Gag proteins in rat cells explain the marked enhancement of p24 accumulation in the medium in spite of the minor increase in *gag* mRNA in the cytoplasm in the presence of hCRM1.

Our finding is reminiscent of HIV-1 replication in murine cells where *gag* mRNA, exported through the CTE/Tap pathway, subsequently restored efficient trafficking of the Gag protein to the plasma membrane, thus underlying the efficient processing and budding of HIV Gag, whereas Gag, translated from mRNA exported via the RRE/Rev/CRM1 pathway, was not targeted to the plasma membrane (Swanson *et al.* 2004). The inefficiency of HIV-1 assembly in murine cells likely reflects a cellular deficiency in the RRE/Rev-dependent nuclear export pathway that is specifically linked to the activation of Gag membrane targeting by the regulatory MA globular-head domain (Sherer *et al.* 2009). Similarly, the trafficking of Gag to the plasma membrane was less efficient in rat cells than human cells, which was substantiated by the immunofluorescent localization of p55 Gag protein to the plasma membrane in rat cells, and was not restored by the presence of hCRM1. Thus, hCRM1 may improve budding process but not membrane trafficking of Gag protein in rat cells.

The results suggest that rCRM1 may export *gag* mRNA into the cytoplasm improperly, resulting in the inefficient processing of Gag proteins. It is most likely that CRM1 has an indirect effect on *gag* mRNA in the cytoplasm, because, upon reaching the cytoplasm, it dissociates from the transport complex containing *gag* mRNA, Rev, Ran and other cellular factors via a mechanism in which RanGTP converts to RanGDP at the periphery of the nuclear pore (Fornerod *et al.* 1997; Fukuda *et al.* 1997; Kudo *et al.* 1997; Neville *et al.* 1997; Ossareh-Nazari *et al.* 1997;

Stade *et al.* 1997). Another cellular factor, Rev-interacting protein (hRIP), also known as hRab or Hrb, which is likely bridged by CRM1, has been reported to function in releasing *gag* mRNA, which would otherwise be trapped at the nuclear periphery, to the cytoplasm (Sanchez-Velar *et al.* 2004; Yu *et al.* 2005). Although, in our hands, *in situ* hybridization did not show improper localization of *gag* mRNA in the cytoplasm of rat cells, it is still possible that aberrant construction of the *gag* mRNA transport complex containing rCRM1 might prevent rat Rip and other cellular factors from functional interactions, finally leading to the inefficient processing of Gag proteins.

Alternatively, cytoplasmic effect of hCRM1 could be attributable to the properties of Gag proteins. Gag has capacities for nuclear entry and RNA binding through its NC region, and RNA promotes multimerization of Gag proteins (Muriaux *et al.* 2001; D'Souza & Summers 2005) that may be an important step of viral particle formation. Thus, it is also conceivable that aberrant RNA complex in rat nucleus may cause inefficient Gag multimerization, leading to reduced viral production.

It is possible that hCRM1 may be needed for correct formation of the complex, which can then interact with rat factors and/or Gag proteins appropriately. Our results indicated that hCRM1 exports *gag* mRNA not only more efficiently than rat CRM1 but also correctly, to the cytoplasm in rat cells, leading to the efficient processing of Gag proteins and HIV-1 particle formation. Our finding that HIV-1 production in rat cells was rescued efficiently by the expression of hCRM1 may have important implications for the development of rat animal models of HIV replication and pathogenesis.

## Experimental procedures

### Cells

Human cell lines, including HeLa, HOS and 293T, and the rat cell lines, ER1/neo1, ER1/hCRM1-7 (Zhang *et al.* 2006), REF52 and W31 (Kanki *et al.* 2000), were maintained in Dulbecco's modified Eagle's medium supplemented with 10% fetal bovine serum in the absence or presence of 300 µg/mL G418 in 10% CO<sub>2</sub> at 37 °C.

### Plasmids

The following plasmids were used in this study: pCMVΔR8.2 (Naldini *et al.* 1996); pCRRE (Kimura *et al.* 1996); pSRαhCRM1 and pSRαrCRM1 (Hakata *et al.* 1998, 2001); pSRα296 (Takebe *et al.* 1988); pSRαtat (Takebe *et al.* 1988);

pCDMβ-gal (Hakata *et al.* 1998); hCRM1-HA and rCRM1-HA, which carried CRM1, fused at the C terminus to an HA tag (Okada *et al.* 2009); pH1-luc (a kind gift from Dr. A. Adachi), which harbors the luciferase gene downstream of the HIV-1 LTR; and pNLmyr(-)pro(-)Flag and pNLmyr(+)-pro(-)Flag (a kind gift from Dr. Y. Morikawa) (Kawada *et al.* 2008).

To construct pSRαhrCRM1-HA and pSRαrhCRM1-HA, the hrCRM1 and rhCRM1 coding regions in pSRαhrCRM1 and pSRαrhCRM1, respectively (Hakata *et al.* 2003), were amplified by PCR using the primer pair for hrCRM1-HA of 5'-GGT CAA TAC CCA CGT TTT TTG AGA GCT CAC TGG A-3' (the underlined sequence is a *SacI* site) and 5'-TAT GGT ACC TTA AGC ATA ATC AGG AAC ATC GTA TGG GTA GTC ACA CAT TTC TTC TGG GAT TTC-3' (the underlined sequence is a *KpnI* site), and the primer pair for rhCRM1-HA of 5'-CTG GAA TCA CTT GGC AGC TGA GCT CTA CAG AGA GAG TCC A-3' (the underlined sequence is a *SacI* site) and 5'-TAT GGT ACC TTA AGC ATA ATC AGG AAC ATC GTA TGG GTA ATC ACA CAT TTC TTC TGG AAT CTC-3' (the underlined sequence is a *KpnI* site.), which encodes the HA tag. The PCR was performed using 10 ng of the plasmid as a template, which was denatured at 94 °C for 2 min and was then followed by 20 cycles of amplification: denaturation (94 °C, 30 s), annealing (62 °C, 1 min) and extension (68 °C, 2 min). A final extension was performed at 68 °C for 10 min. The amplified DNA was digested with *SacI* and *KpnI*, and inserted into these sites in pSRαhrCRM1 or pSRαrhCRM1, as appropriate.

### Real-time RT-PCR

To separate the cytoplasmic and nuclear fractions, lysis buffer (0.5% NP40, 10 mM Tris-HCl [pH 7.4], 0.14 M NaCl, 1.5 mM MgCl<sub>2</sub>, 1 U/µL RNase Inhibitor (TOYOBO), 1 mM DTT) was added to the cell pellets and the lysates were centrifuged in a microcentrifuge at 500 × *g* for 5 min at 4 °C. Total RNA in the cytoplasm (supernatant) and nucleus (pellet) was extracted using the Absolutely RNA Miniprep Kit (Stratagene). The ThermoScript RT-PCR System (Invitrogen) was used to synthesize cDNAs from 150 to 500 ng of RNA, and the abundance was quantified using real-time PCR with a Light Cycler PCR machine (Roche). PCRs were performed using the following primer pairs: *gag* forward (5'-AGA GAA GGC TTT CAG CCC AGA AGT-3') and reverse (5'-GGA TTT GTT ACT TGG CTC ATT GCT-3'); *tat* forward (5'-GTG GAA GCA TCC AGG AAG TCA GCC-3') and reverse (5'-CTA TTC CTT CGG GCC TGT CGG GTC-3'); and *β-gal* forward (5'-GCG AAT ACC TGT TCC G-3') and reverse (5'-GCG TCA CAC TGA GGT T-3'). PCR mixtures (20 µL) were prepared in a capillary tube containing 1/16 of the volume of the RT reaction mixture, each primer pair (0.5 µM) and 1 × Light Cycler-FastStart SYBR Green PCR Master Mix. After an initial Taq polymerase activation step (95 °C, 15 min), the *gag* and *tat* mRNA amplification reactions were performed using 40 cycles of denaturation (95 °C, 10 s), annealing (68 °C, 10 s) and extension (72 °C, 15 s),

whereas the  $\beta$ -gal mRNA was amplified using 40 cycles of denaturation (95 °C, 15 s), annealing (60 °C, 5 s) and extension (72 °C, 11 s). The abundance of each mRNA was estimated with a standard regression curve using the Light Cycler Software v. 3 (Roche). The standard curve was obtained by PCR amplification of 0.0064–500 pg of pCMV $\Delta$ R8.2 (for *gag* mRNA), pSR $\alpha$ tat and pCDM $\beta$ -gal.

To ascertain the efficiency of fractionation,  $\beta$ -actin pre-mRNA was amplified by PCR using the primers  $\beta$ -actin-F (5'-TCG ATC GCC TTT CTG ACT AGG TG-3') and  $\beta$ -actin-R (5'-GGT CAG GAT CTT CAT GAG GTA GTC TG-3'); the former targets the intron and the latter targets the exon of  $\beta$ -actin pre-mRNA. Reactions were performed with 25 cycles of denaturation at 94 °C for 30 s, followed by annealing at 59 °C for 1 min and extension at 72 °C for 30 s.

### Pulse chase assay

At 36 to 48 h post-transfection, cells were metabolically labeled with an [<sup>35</sup>S] methionine/cysteine mixture (GE Healthcare UK Ltd.) for 30 min. Cells were washed once and then chased for 0, 4, 8 and 24 h in 1 mL of medium supplemented with 10  $\mu$ M methionine, 10  $\mu$ M cysteine and 100 nM KNI-272 (an HIV-1 protease inhibitor, the kind gift of Dr. Y. Kiso). After chasing, 0.25 mL of 5 $\times$  detergent buffer containing 2.5% deoxycholate, 2.5% Triton  $\times$ 100, 250 mM Tris-HCl (pH 7.6), 0.1 M NaCl, 0.1 M EDTA, 100 nM KNI-272 and a protease inhibitor cocktail (Roche) was added to the culture to dissolve Gag proteins in both the medium and cells. The lysates were centrifuged in a microcentrifuge at 7200  $\times$  g for 15 min, and the supernatant was incubated with anti-Gag mAb V107 (Ikuta *et al.* 1989) (a kind gift from Dr. K. Ikuta) for 1 h at 4 °C, followed by incubation with protein-G Sepharose for 1 h at 4 °C. After three washes with detergent buffer, the precipitated complexes were analyzed by SDS-PAGE and autoradiography.

At 40 h post-transfection with pNLmyr(-)pro(-)Flag, cells were metabolically labeled with an [<sup>35</sup>S]-methionine/cysteine mixture for 15 min, washed and then chased for 0, 4 and 7 h as described earlier. The detergent buffer (0.5 mL) was added to the cells and centrifuged in a microcentrifuge at 7200  $\times$  g for 15 min. The supernatant was incubated with anti-Flag M2 antibody (Sigma) conjugated to protein-G Sepharose for 3 h at 4 °C, followed by three washes with the detergent buffer.

### In situ hybridization

At 48 to 50 h after transfection, cells were subjected to an *in situ* hybridization assay, which has been described previously (Tautz & Pfeifle 1989; Kimura *et al.* 1996). Probes were prepared by PCR amplification of a 167-bp fragment from HIV-1 *gag* using the primers T66 (5'-GAGAGCGTCGGT ATTAAG-3'; HIV-1<sub>NL4-3</sub> nts 798–815) and T67 (5'-GTC TACAGCCTTCTGATG-3'; HIV-1<sub>NL4-3</sub> nts 964–947). The fragment generated was then used as a template for a second PCR, using either T67 or T66 primers and the digoxigenin (DIG)-nucleotide mixture (Roche), essentially as described by

Tautz & Pfeifle (1989). Cells were examined under a confocal laser-scanning microscope (Olympus).

### Western blotting

The transfected cells were dissolved in TMN buffer containing 10 mM Tris-HCl (pH 7.4), 2 mM MgCl<sub>2</sub>, 0.5% NP40 and a protease inhibitor cocktail. After measuring the  $\beta$ -gal activity and protein levels, the proteins were solubilized with sample buffer and resolved by SDS-PAGE and then transferred to a nitrocellulose filter. V107, a rat anti-HA mAb (Roche), a rabbit anti- $\beta$ -gal Ab, a mouse anti-actin mAb and anti-FLAG M2 Ab were used as primary Abs. Horseradish peroxidase-conjugated anti-IgG Abs (Promega) were used as secondary Abs. Immuno-reactive bands were visualized using ECL + plus (GE Health care) followed by the LAS-1000 Plus system (Fujifilm) and were evaluated by Image Gauge (version 3.4) software (Fujifilm).

### Immunofluorescence

Subconfluent ER1/neo1 cells, seeded onto coverslips (Fisher Scientific) in six-well plates, were transfected using Polyethylenimine 'Max' (PEI) (Polyscience) and fixed 18 h post-transfection with 2% paraformaldehyde dissolved in PBS. The cells were then permeabilized with 0.5% NP40 in PBS and incubated with blocking solution (5% skim milk in PBS) for 1 h at RT. The cells were stained with Alexa Fluor488-conjugated anti-HA-Tag (6E2) mouse mAb and Alexa Fluor<sup>®</sup> 555-conjugated anti-DYKDDDDK (FLAG) Tag antibody (Cell Signaling Technology) for 1 h at RT, washed and then mounted with VECTASHIELD Hard set Mounting Medium (Vector Laboratories). The stained cells were examined under a confocal laser-scanning microscope.

### Preparation of VLP

To prepare the viral-like particle (VLP) fraction, medium from the cell cultures was centrifuged at 530  $\times$  g for 10 min and the supernatant was filtered through a Millex HV 0.45  $\mu$ m Filter Unit (Millipore). The HIV-1 particles were pelleted through a 20% (W/V) sucrose solution by centrifugation at 86,000  $\times$  g in an SW28 rotor for 2 h at 4 °C.

### Statistical analysis

Comparisons between individual data points were made using a Student's *t*-test. Two-sided *P*-values  $\leq$  0.05 were considered statistically significant.

### Acknowledgements

We thank Dr J. Fujisawa for kind administration, and K. Ofuji, A. Hirano, N. Mizuno and S. Yamanouchi for excellent technical assistance. V107, pH1-luc, pNLmyr(-)pro(-)Flag, and KNI-272 were kind gifts from Dr K. Ikuta (University of

Osaka), Dr A. Adachi (Tokushima University), Dr Y. Morikawa (Kitazato University) and Dr Y. Kiso (Kyoto Pharmaceutical University), respectively. This study was supported by grants from the Ministry of Sports and Culture (Japan) and the Ministry of Health and Welfare (Japan).

## References

- Bieniasz, P.D. & Cullen, B.R. (2000) Multiple blocks to human immunodeficiency virus type 1 replication in rodent cells. *J. Virol.* **74**, 9868–9877.
- Browning, J., Horner, J.W., Pettoello-Mantovani, M., Raker, C., Yurasov, S., DePinho, R.A. & Goldstein, H. (1997) Mice transgenic for human CD4 and CCR5 are susceptible to HIV infection. *Proc. Natl Acad. Sci. USA* **94**, 14637–14641.
- Cullen, B.R. (1998) Retroviruses as model systems for the study of nuclear RNA export pathways. *Virology* **249**, 203–210.
- Cullen, B.R. (2003) Nuclear RNA export. *J. Cell Sci.* **116**, 587–597.
- D'Souza, V. & Summers, M.F. (2005) How retroviruses select their genomes. *Nat. Rev. Microbiol.* **3**, 643–655.
- Formerod, M., Ohno, M., Yoshida, M. & Mattaj, I.W. (1997) CRM1 is an export receptor for leucine-rich nuclear export signals. *Cell* **90**, 1051–1060.
- Fukuda, M., Asano, S., Nakamura, T., Adachi, M., Yoshida, M., Yanagida, M. & Nishida, E. (1997) CRM1 is responsible for intracellular transport mediated by the nuclear export signal. *Nature* **390**, 308–311.
- Giuffre, A.C., Higgins, J., Buckheit, R.W. Jr & North, T.W. (2003) Susceptibilities of simian immunodeficiency virus to protease inhibitors. *Antimicrob. Agents Chemother.* **47**, 1756–1759.
- Goffinet, C., Michel, N., Allespach, I., Tervo, H.M., Hermann, V., Krausslich, H.G., Greene, W.C. & Keppler, O.T. (2007) Primary T-cells from human CD4/CCR5-transgenic rats support all early steps of HIV-1 replication including integration, but display impaired viral gene expression. *Retrovirology* **4**, 53.
- Hakata, Y., Umemoto, T., Matsushita, S. & Shida, H. (1998) Involvement of human CRM1 (exportin 1) in the export and multimerization of the Rex protein of human T-cell leukemia virus type 1. *J. Virol.* **72**, 6602–6607.
- Hakata, Y., Yamada, M., Mabuchi, N. & Shida, H. (2002) The carboxy-terminal region of the human immunodeficiency virus type 1 protein Rev has multiple roles in mediating CRM1-related Rev functions. *J. Virol.* **76**, 8079–8089.
- Hakata, Y., Yamada, M. & Shida, H. (2001) Rat CRM1 is responsible for the poor activity of human T-cell leukemia virus type 1 Rex protein in rat cells. *J. Virol.* **75**, 11515–11525.
- Hakata, Y., Yamada, M. & Shida, H. (2003) A multifunctional domain in human CRM1 (exportin 1) mediates RanBP3 binding and multimerization of human T-cell leukemia virus type 1 Rex protein. *Mol. Cell. Biol.* **23**, 8751–8761.
- Hazuda, D.J., Young, S.D., Guare, J.P., *et al.* (2004) Integrase inhibitors and cellular immunity suppress retroviral replication in rhesus macaques. *Science* **305**, 528–532.
- Hu, S.L. (2005) Non-human primate models for AIDS vaccine research. *Curr. Drug Targets Infect. Disord.* **5**, 193–201.
- Ikuta, K., Morita, C., Miyake, S., Ito, T., Okabayashi, M., Sano, K., Nakai, M., Hirai, K. & Kato, S. (1989) Expression of human immunodeficiency virus type 1 (HIV-1) gag antigens on the surface of a cell line persistently infected with HIV-1 that highly expresses HIV-1 antigens. *Virology* **170**, 408–417.
- Kanki, K., Torigoe, T., Hirai, I., Sahara, H., Kamiguchi, K., Tamura, Y., Yagihashi, A. & Sato, N. (2000) Molecular cloning of rat NK target structure—the possibility of CD44 involvement in NK cell-mediated lysis. *Microbiol. Immunol.* **44**, 1051–1061.
- Kawada, S., Goto, T., Haraguchi, H., Ono, A. & Morikawa, Y. (2008) Dominant negative inhibition of human immunodeficiency virus particle production by the nonmyristoylated form of gag. *J. Virol.* **82**, 4384–4399.
- Keppler, O.T., Welte, F.J., Ngo, T.A., *et al.* (2002) Progress toward a human CD4/CCR5 transgenic rat model for de novo infection by human immunodeficiency virus type 1. *J. Exp. Med.* **195**, 719–736.
- Keppler, O.T., Yonemoto, W., Welte, F.J., Patton, K.S., Iacovides, D., Atchison, R.E., Ngo, T., Hirschberg, D.L., Speck, R.F. & Goldsmith, M.A. (2001) Susceptibility of rat-derived cells to replication by human immunodeficiency virus type 1. *J. Virol.* **5**, 8063–8073.
- Kimura, T., Hashimoto, I., Nishikawa, M. & Fujisawa, J.I. (1996) A role for Rev in the association of HIV-1 gag mRNA with cytoskeletal beta-actin and viral protein expression. *Biochimie* **78**, 1075–1080.
- Kudo, N., Khochbin, S., Nishi, K., Kitano, K., Yanagida, M., Yoshida, M. & Horinouchi, S. (1997) Molecular cloning and cell cycle-dependent expression of mammalian CRM1, a protein involved in nuclear export of proteins. *J. Biol. Chem.* **272**, 29742–29751.
- Malim, M.H. & Cullen, B.R. (1991) HIV-1 structural gene expression requires the binding of multiple Rev monomers to the viral RRE: implications for HIV-1 latency. *Cell* **65**, 241–248.
- Malim, M.H., McCarn, D.F., Tiley, L.S. & Cullen, B.R. (1991) Mutational definition of the human immunodeficiency virus type 1 Rev activation domain. *J. Virol.* **65**, 4248–4254.
- Marques, S.M., Veyrone, J.L., Shukla, R.R. & Kumar, A. (2003) Restriction of human immunodeficiency virus type 1 Rev function in murine A9 cells involves the Rev C-terminal domain. *J. Virol.* **77**, 3084–3090.
- Muriaux, D., Mirro, J., Harvin, D. & Rein, A. (2001) RNA is a structural element in retrovirus particles. *Proc. Natl Acad. Sci. USA* **98**, 5246–5251.
- Nakiely, S. & Dreyfuss, G. (1999) Transport of proteins and RNAs in and out of the nucleus. *Cell* **99**, 677–690.
- Naldini, L., Blomer, U., Gally, P., Ory, D., Mulligan, R., Gage, F.H., Verma, I.M. & Trono, D. (1996) *In vivo* gene

- delivery and stable transduction of nondividing cells by a lentiviral vector. *Science* **272**, 263–267.
- Neville, M., Stutz, F., Lee, L., Davis, L.I. & Rosbash, M. (1997) The importin-beta family member Crm1p bridges the interaction between Rev and the nuclear pore complex during nuclear export. *Curr. Biol.* **7**, 767–775.
- Okada, H., Zhang, X., Fofana, I.B., Nagai, M., Suzuki, H., Ohashi, T. & Shida, H. (2009) Synergistic effect of human CytT1 and CRM1 on HIV-1 propagation in rat T cells and macrophages. *Retrovirology* **6**, 43.
- Ossareh-Nazari, B., Bachelier, F. & Dargemont, C. (1997) Evidence for a role of CRM1 in signal-mediated nuclear protein export. *Science* **278**, 141–144.
- Sanchez-Velar, N., Udofia, E.B., Yu, Z. & Zapp, M.L. (2004) hRIP, a cellular cofactor for Rev function, promotes release of HIV RNAs from the perinuclear region. *Genes Dev.* **18**, 23–34.
- Sherer, N.M., Swanson, C.M., Papaioannou, S. & Malim, M.H. (2009) Matrix mediates the functional link between human immunodeficiency virus type 1 RNA nuclear export elements and the assembly competency of Gag in murine cells. *J. Virol.* **83**, 8525–8535.
- Shultz, L.D., Ishikawa, F. & Greiner, D.L. (2007) Humanized mice in translational biomedical research. *Nat. Rev. Immunol.* **7**, 118–130.
- Stade, K., Ford, C.S., Guthrie, C. & Weis, K. (1997) Exportin 1 (Crm1p) is an essential nuclear export factor. *Cell* **90**, 1041–1050.
- Swanson, C.M., Puffer, B.A., Ahmad, K.M., Doms, R.W. & Malim, M.H. (2004) Retroviral mRNA nuclear export elements regulate protein function and virion assembly. *The EMBO J.* **23**, 2632–2640.
- Takayanagi, R., Ohashi, T., Yamashita, E., Kurosaki, Y., Tanaka, K., Hakata, Y., Komoda, Y., Ikeda, S., Tsunetsugu-Yokota, Y., Tanaka, Y. & Shida, H. (2007) Enhanced replication of human T-cell leukemia virus type 1 in T cells from transgenic rats expressing human CRM1 that is regulated in a natural manner. *J. Virol.* **81**, 5908–5918.
- Takebe, Y., Seiki, M., Fujisawa, J., Hoy, P., Yokota, K., Arai, K., Yoshida, M. & Arai, N. (1988) SR alpha promoter: an efficient and versatile mammalian cDNA expression system composed of the simian virus 40 early promoter and the R-U5 segment of human T-cell leukemia virus type 1 long terminal repeat. *Mol. Cell. Biol.* **8**, 466–472.
- Tautz, D. & Pfeifle, C. (1989) A non-radioactive *in situ* hybridization method for the localization of specific RNAs in *Drosophila* embryos reveals translational control of the segmentation gene hunchback. *Chromosoma* **98**, 81–85.
- Trono, D. & Baltimore, D. (1990) A human cell factor is essential for HIV-1 Rev action. *EMBO J.* **9**, 4155–4160.
- Veazey, R.S., Klasse, P.J., Schader, S.M., Hu, Q., Ketas, T.J., Lu, M., Marx, P.A., Dufour, J., Colonna, R.J., Shattock, R.J., Springer, M.S. & Moore, J.P. (2005) Protection of macaques from vaginal SHIV challenge by vaginally delivered inhibitors of virus-cell fusion. *Nature* **438**, 99–102.
- Watanabe, S., Terashima, K., Ohta, S., Horibata, S., Yajima, M., Shiozawa, Y., Dewan, M.Z., Yu, Z., Ito, M., Morio, T., Shimizu, N., Honda, M. & Yamamoto, N. (2007) Hematopoietic stem cell-engrafted NOD/SCID/IL2R-gamma null mice develop human lymphoid systems and induce long-lasting HIV-1 infection with specific humoral immune responses. *Blood* **109**, 212–218.
- Yu, Z., Sanchez-Velar, N., Catrina, I.E., Kittler, E.L., Udofia, E.B. & Zapp, M.L. (2005) The cellular HIV-1 Rev cofactor hRIP is required for viral replication. *Proc. Natl Acad. Sci. USA* **102**, 4027–4032.
- Zhang, X., Hakata, Y., Tanaka, Y. & Shida, H. (2006) CRM1, an RNA transporter, is a major species-specific restriction factor of human T cell leukemia virus type 1 (HTLV-1) in rat cells. *Microbes Infect.* **8**, 851–859.
- Zheng, Y.H., Yu, H.F. & Peterlin, B.M. (2003) Human p32 protein relieves a post-transcriptional block to HIV replication in murine cells. *Nat. Cell Biol.* **5**, 611–618.

Received: 2 October 2010

Accepted: 1 November 2010

## Supporting Information/Supplementary material

The following Supporting Information can be found in the online version of the article:

**Figure S1** Polyribosome profile analysis of *gag*, *tat* and *b-gal* mRNAs in the presence or absence of hCRM1.

**Data S1** Materials and method.

Additional Supporting Information may be found in the online version of this article.

Please note: Wiley-Blackwell are not responsible for the content or functionality of any supporting materials supplied by the authors. Any queries (other than missing material) should be directed to the corresponding author for the article.



Original article

# Inhibitory effect of human TRIM5 $\alpha$ on HIV-1 production

Xianfeng Zhang<sup>a</sup>, Mariko Kondo<sup>a,1</sup>, Jing Chen<sup>a</sup>, Hiroyuki Miyoshi<sup>b</sup>, Hajime Suzuki<sup>a</sup>, Takashi Ohashi<sup>a</sup>, Hisatoshi Shida<sup>a,\*</sup>

<sup>a</sup> Institute for Genetic Medicine, Hokkaido University, Kita-15, Nishi-7, Kita-ku, Sapporo 060-0815, Japan

<sup>b</sup> Subteam for Manipulation of Cell Fate, RIKEN BioResource Center, Tsukuba, Ibaraki 305-0074, Japan

Received 27 January 2010; accepted 11 May 2010

Available online 21 May 2010

## Abstract

Tripartite motif-containing 5 isoform- $\alpha$  (TRIM5 $\alpha$ ), a host restriction factor, blocks infection of some retroviruses at a post-entry, pre-integration stage in a species-specific manner. A recent report by Sakuma et al. describes a second antiretroviral activity of rhesus macaque TRIM5 $\alpha$ , which blocks HIV-1 production through rapid degradation of HIV-1 Gag polyproteins. Here, we find that human TRIM5 $\alpha$  limits HIV-1 production. Transient expression of TRIM5 $\alpha$  decreased HIV-1 production, whereas knockdown of TRIM5 $\alpha$  in human cells increased virion release. A single amino acid substitution (R437C) in the SPRY domain diminished the restriction effect. Moderate levels of human wild-type TRIM5 $\alpha$  and a little amount of R437C mutant were incorporated into HIV-1 virions. The R437C mutant also lost restriction activity against N-tropic murine leukemia virus infection. However, the corresponding R to C mutation in rhesus macaque TRIM5 $\alpha$  had no effect on the restriction ability. Our findings suggest human TRIM5 $\alpha$  is an intrinsic immunity factor against HIV-1 infection. The importance of arginine at 437 aa in SPRY domain for the late restriction is species-specific.

© 2010 Elsevier Masson SAS. All rights reserved.

**Keywords:** Human TRIM5 $\alpha$ ; HIV-1 production; Restriction factor; Intrinsic immunity; MLV

## 1. Introduction

The intrinsic host defense system has recently come to light as a key player in restricting retroviral infection. Several intrinsic factors important in limiting HIV-1 infection have been identified. APOBEC3G [1] and APOBEC3F [2] interfere with the replication of HIV-1 and other retroviruses via their cytidine deaminase activity [3,4]. The membrane protein Tetherin blocks the release of HIV-1 and other enveloped viruses by tethering them to the cellular membrane [5]. TRIM5 $\alpha$  has been shown to be a post-entry restriction factor that confers resistance to

HIV-1 in a species-specific manner. Even though these restriction factors are thought to be constitutively expressed and active before pathogen invasion [6,7], they are induced by interferon and therefore may constitute innate immune defenses [5,8,9].

TRIM5 $\alpha$  has been proposed to bind the incoming viral capsid and interfere with uncoating [10,11]. It has also been reported that TRIM5 $\alpha$  possesses E3 ubiquitin ligase activity and a mutation in its RING finger domain decreases its restriction ability [12–14]. Other reports suggest that TRIM5 $\alpha$  prevents late RT product formation and inhibits viral cDNA nuclear import [15,16].

Recently, another antiretroviral activity of TRIM5 $\alpha$  of rhesus monkey, TRIM5 $\alpha_{rh}$ , has been described, which is inhibition of HIV-1 production at a post-translational stage by degradation of the Gag protein [17]. SIV is resistant to this restriction. However, another group argued against this effect of TRIM5 $\alpha_{rh}$  [18] although both showed that overexpression of TRIM5 $\alpha_{rh}$  down-regulates HIV-1 production.

\* Corresponding author. Institute for Genetic Medicine, Hokkaido University, Kita-15, Nishi-7, Kita-ku, Sapporo 060-0815, Japan. Tel./fax: +81 11 706 7543.

E-mail address: hshida@igm.hokudai.ac.jp (H. Shida).

<sup>1</sup> Present address: Mylan Seiyaku Ltd. Holland Hills Mori Tower 15F, 5-11-2 Toranomon, Minato-ku, Tokyo 105-0001, Japan.

TRIM5 $\alpha$  is a member of the tripartite motif protein family and contains RING, B-box 2, and coiled-coil domains, as well as a carboxy-terminal B30.2 (SPRY) domain. The contribution of each domain to HIV-1 post-entry restriction had been well documented. The RING domain contributes to the potency of restriction but is not absolutely essential. The B-box 2, coiled-coil and SPRY domains of TRIM5 $\alpha$  are necessary for anti-retroviral activity. The coiled-coil domain is indispensable for TRIM5 $\alpha$  oligomerization, which increases the avidity of TRIM5 $\alpha$  for the retroviral capsid. Both the coiled-coil and SPRY domains are essential for TRIM5 $\alpha$  to bind the virion core [19]. Variation in the SPRY domain is thought to be responsible for species-specific differences in retroviral restriction [19,20]. During the study for the late-restriction, the RING structure and B-box 2, coiled-coil and ensuing linker 2 domains are all found to be responsible, while the N-terminal region, RING and B-box2 domains have been shown to be essential for interaction between TRIM5 $\alpha_{rh}$  and HIV-1 Gag. The coiled-coil domain and linker 2 region may play an effector function in late-restriction as well as the known effect on formation of the cytoplasmic body including TRIM5 $\alpha_{rh}$  [21].

Human TRIM5 $\alpha$  (TRIM5 $\alpha_{hu}$ ) had been considered to have no antiviral activity on HIV-1 production. However, during the course of our study comparing the TRIM5s of various species including primate TRIM5 $\alpha$  and rodent TRIM5, we do find that TRIM5 $\alpha_{hu}$  potently blocked the release of HIV-1 when expressed at the same level with TRIM5 $\alpha_{rh}$ . Here, we provide the evidences that TRIM5 $\alpha_{hu}$  inhibits production of HIV-1 progeny at physiological concentrations, suggesting it plays an important role in intrinsic defense against HIV-1.

## 2. Materials and methods

### 2.1. Cell culture

Human 293T, HeLa, HT1080, TZM-bl [22] and Plat-gp cells [23] were maintained in DMEM containing 10% FCS and antibiotics. Jurkat E6-1 cells (ATCC number: TIB-152) were cultured in RPMI1640 containing 10% FCS.

### 2.2. Plasmids

The plasmid pRhT5 $\alpha$ , which encodes C-terminal hemagglutinin (HA)-tagged TRIM5 $\alpha_{rh}$ , was provided by Dr. Ikeda. The plasmid encoding HA-tagged TRIM5 $\alpha_{hu}$  was obtained from Dr. Shioda, and designated pHuT5 $\alpha$ WT. HA-tagged TRIM5 $\alpha_{hu}$  cDNA harboring the R437C mutation was amplified by RT-PCR from human peripheral blood mononuclear cells (PBMC) with a previously described primer pair [17], and kindly provided by Dr. Y. Ikeda. It was then cloned into pcDNA3.1 (Invitrogen), the same vector that was used to generate pRhT5 $\alpha$  and pHuT5 $\alpha$ WT. The resultant plasmid was designated pHuT5 $\alpha$ R437C. For construction of pRhT5 $\alpha$ R441C, a corresponding mutant of TRIM5 $\alpha_{hu}$ R437C, the plasmid pRhT5 $\alpha$  was used as a template for QuikChange site-directed mutagenesis (Stratagene). To generate TRIM5 $\alpha$

encoding retroviruses, the retroviral vector pMX-puro [24] and Plat-gp packaging cells were used. The HA-tagged TRIM5 $\alpha$  open reading frames (ORFs) described above were amplified by PCR using primers huT5 $\alpha$ -F-EcoRI (5'-GCGAATTCCACCATGGCTTCTGGAATCCTG-3'; Underline shows EcoRI site.) and NotI-HA-R (5'-AGATAA-GAATGCGGCCGCTCAAGCGTAATCTGGAACATCG-3'; Underline shows NotI site.) and then cloned into EcoRI and NotI sites of pMX-puro. The resulting plasmid was designated pMX-T5 $\alpha$ -HA-puro. All of the TRIM5 $\alpha$  proteins possess a carboxy-terminal HA tag to allow detection of the expression level. The HIV-1 molecular clone pNL $\Delta$ poIEGFP was constructed by inserting the EGFP ORF in the Nef coding region of pNL $\Delta$ pol [25] that lacks a 328 base pair fragment in the polymerase coding region of pNL4-3 [26]. The resultant plasmid produces the p55 Gag precursor protein that is processed to p24 capsid protein. The plasmid of pYK-JRCSF [27], pNL4-3, pSIVmac239 [28], pSA212, encoding full length genome of SIVagm [29] and p89.6 [30], were obtained from Dr. Y. Koyanagi, Dr. Adachi, Dr. Mori, Dr. Miura, and AIDS Research and Reference Reagent Program, respectively. The  $\beta$ -galactosidase ( $\beta$ -gal) expression plasmid pCDM- $\beta$ -gal [31] was used.

### 2.3. Transfection and viral infection

Co-transfection of one of pNL $\Delta$ poIEGFP, pYK-JRCSF, pNL4-3, p89.6, pSA212 and pSIVmac239 with TRIM5 $\alpha$  expression plasmids (pRhT5 $\alpha$ , pHuT5 $\alpha$ WT, pHuT5 $\alpha$ R437C) or empty vector pcDNA3.1 into 293T cells was carried out using Lipofectamine and Plus reagent (Invitrogen) according to the manufacturer's instructions. Two days later, the culture supernatants were harvested and the p24 concentration was measured with p24 Gag ELISA assay kit (Zeptmatrix). The p24 concentration was divided by intracellular  $\beta$ -gal activity evaluated by standard colorimetric methods. The value of control pcDNA3.1-transfected cells was set as 1, and compared with the value of various TRIM5 $\alpha$  expression plasmid-transfected cells.

To measure the infectivity of progeny viruses, TZM-bl cells, the HeLa cell derivatives that express human CD4 and CCR5 and contain a luciferase construct under the control of the HIV-1 promoter, were seeded in 24-well plate ( $5 \times 10^4$ /well). The next day, the medium was removed and the cells were incubated with 250  $\mu$ l of HIV-1 or SIV harboring culture media for 3.5 h followed by adding 750  $\mu$ l of fresh media. Forty-eight hours after infection, cells were washed and lysed, and then luciferase activity was measured using Promega's BrightGlo luciferase assay system. To calculate the production rate of infectious virus, the ratio of luciferase activities against the  $\beta$ -gal activities in HIV-1/SIV producing 293T cell lysates was calculated and the value of control pcDNA3.1-transfected sample was set as 1.

### 2.4. Preparation of viral like particle (VLP)

The culture supernatants (2 ml) were harvested 48 h post-transfection, and cellular debris was removed by centrifugation

at 2000 rpm (Himac CF 7D2, HITACHI) for 20 min, followed by filtration of the supernatants through 0.45- $\mu$ m pore size syringe filters (Millipore). The supernatants (1 ml) were then concentrated by ultracentrifugation through a 20% (w/v in PBS) sucrose cushion for 2 h at 45 000 rpm (TLA100.4 rotor; Beckman) at 4 °C. The pellets were resuspended in 15  $\mu$ l of lysis buffer (10 mM Tris–HCl (pH 7.4), 1 mM MgCl<sub>2</sub>, 140 mM NaCl, 0.5% NP-40, and protease inhibitors (Roche)) and analyzed by Western blotting.

### 2.5. Generation of cells stably expressing TRIM5 $\alpha$ variants

Recombinant retroviruses encoding various TRIM5 $\alpha$  were produced in Plat-gp cells by co-transfecting constructed retroviral vector plasmids which encoded a TRIM5 $\alpha$  ORF (pMX-huT5 $\alpha$ WT-HA-puro, pMX-huT5 $\alpha$ R437C-HA-puro, pMX-rhT5 $\alpha$ -HA-Puro, pMX-agmT5 $\alpha$ -HA-Puro) and pMD.G [32], a plasmid encoding the vesicular stomatitis virus (VSV) G envelope glycoprotein. Forty-eight hours post-transfection, the culture supernatants were harvested and then transduced to 293T or HeLa cells ( $2 \times 10^5$ ) in the presence of 10  $\mu$ g/ml of polybrene. Cells were then selected in medium containing 2  $\mu$ g/ml puromycin (Sigma).

### 2.6. Production and infection of pseudoviruses

VSV-G-coated HIV-1 pseudovirus expressing Venus (HIV-1-Venus) was prepared by transfecting 293T cells with a combination of CSII-EF-MCS-IRES2-Venus, pMDLg/pRRE, pMD.G and pRSV-Rev [32]. One day after transfection, culture medium was replaced with fresh DMEM containing 10% FCS, 1% non-essential amino acid, 1 mM sodium pyruvate, 10  $\mu$ M forskolin and antibiotics. Two days later, the culture medium was collected, filtered through 0.45  $\mu$ m filter membrane and frozen at –80 °C. N-tropic and B-tropic murine leukemia viruses (MLVs) were generated by co-transfecting 3 plasmids (pLNCX-GFP, pMD.G, and pCIGS-N or pCIGS-B) [33] into 293T cells. Forty-eight hours post-transfection, the culture media was harvested and stored at –80 °C.

VSV-G-pseudotyped HIV-1-Venus was infected in the presence of 10  $\mu$ g/ml of polybrene to HeLa cells that had been transduced with various TRIM5 $\alpha$  encoding retroviruses followed by selection in the presence of puromycin for 3 days. Forty-eight hours post-infection, the cells were harvested, washed once with PBS, fixed with PBS containing 1% formaldehyde and then subjected to fluorescence-activated cell sorting (FACS) analysis with a FACScalibur (Becton Dickinson).

### 2.7. Immunoblotting

The cells were harvested in the lysis buffer as described above. The primary antibody for detection of the HA tag was anti HA 3F10 (Roche). HIV-1 p55/p24 Gag protein was detected using a murine anti-p24 mAb (V107 [34], a kind gift

of Dr. K. Ikuta). The amount of cell lysates analyzed by SDS-PAGE was normalized by  $\beta$ -gal activity. The bands were visualized by ECL western blotting system (GE healthcare). The intensity of bands was quantified using LAS 1000 mini (Fuji film) when necessary.

### 2.8. Reduction of Trim5 $\alpha$ expression by siRNA

A mixture of siRNAs (B-bridge international, Inc) against TRIM5 $\alpha$ <sub>hu</sub> with the target sequences 5'-CCUGAGAA-CAUACGGCCUAdTdT-3', 5'-GAGAAAGCUUCCUGGAA-GAdTdT-3' and 5'-CUGAAAAGCCUUACGAACUdTdT-3' were co-transfected into  $5 \times 10^4$  HT1080 and  $1 \times 10^5$  293T cells at a final concentration of 50 nM together with 0.01  $\mu$ g of pNL $\Delta$ poIEGFP using Lipofectamine2000 (Invitrogen). Jurkat E6-1 cells ( $2 \times 10^6$ ) were electroporated with 50 pmol of anti-TRIM5 $\alpha$ <sub>hu</sub> or control siRNA and 0.2  $\mu$ g of pNL $\Delta$ poIEGFP by nucleofection (Amaxa) using cell line nucleofector kit V and the program X-01.

### 2.9. RT-PCR

Total RNA from siRNA-transfected cells was isolated using the Absolutely RNA kit (Stratagene) according to the manufacturer's instructions. First-strand cDNA was synthesized using 0.5  $\mu$ g total RNA in a 20  $\mu$ l reaction volume with the ThermoScript First-Strand Synthesis System (Invitrogen), and the product was subjected to PCR using primers for TRIM5 $\alpha$  (forward: 5'-TGGAAGACTCAAATACAGTATGACAA-3'; reverse: 5'-CATCTAGTTTCAGAGTTCGTAAG-3') and for human G3PDH (forward: 5'-AAA TGA GCT TGA CAA AGT GGT CG-3'; reverse: 5'-GTA TGA CAA CAG CCT CAA GAT CA-3') as an internal control. In parallel, the TRIM5 $\alpha$  cDNA was quantified by lightCycler (Roche) realtime PCR.

## 3. Results

### 3.1. Effect of TRIM5 $\alpha$ <sub>hu</sub> on HIV-1 production

While investigating whether TRIM5 $\alpha$  from various species exhibited intrinsic immunity against HIV-1 infection, we used two TRIM5 $\alpha$ <sub>hu</sub> clones as controls. Unexpectedly over-expression of one of TRIM5 $\alpha$ <sub>hu</sub> clone in human 293T cells reduced HIV-1 p24 Gag production and the other did not. After sequencing the two human TRIM5 $\alpha$ s, we found a mutation from arginine to cysteine at amino acid (a.a.) 437 in the latter TRIM5 $\alpha$  clone (Fig. 1A, plasmid pHuT5 $\alpha$ R437C).

To directly compare the effect of wild type and mutant TRIM5 $\alpha$ <sub>hu</sub> and TRIM5 $\alpha$ <sub>rh</sub> on HIV-1 production, we transfected 293T cells with the HIV-1 molecular clone pNL $\Delta$ poIEGFP together with varying amounts of C-terminal HA-tagged TRIM5 $\alpha$  encoding plasmids (pHuT5 $\alpha$ WT, pRhT5 $\alpha$  and pHuT5 $\alpha$ R437C). Then we evaluated the p24 levels in the culture supernatants. As shown in Fig. 1B, the production of p24 was not blocked by expression of the TRIM5 $\alpha$ <sub>hu</sub> R437C mutant, but was markedly suppressed by TRIM5 $\alpha$ <sub>hu</sub> wild type and TRIM5 $\alpha$ <sub>rh</sub> in a dose dependent manner. TRIM5 $\alpha$ <sub>rh</sub> looked

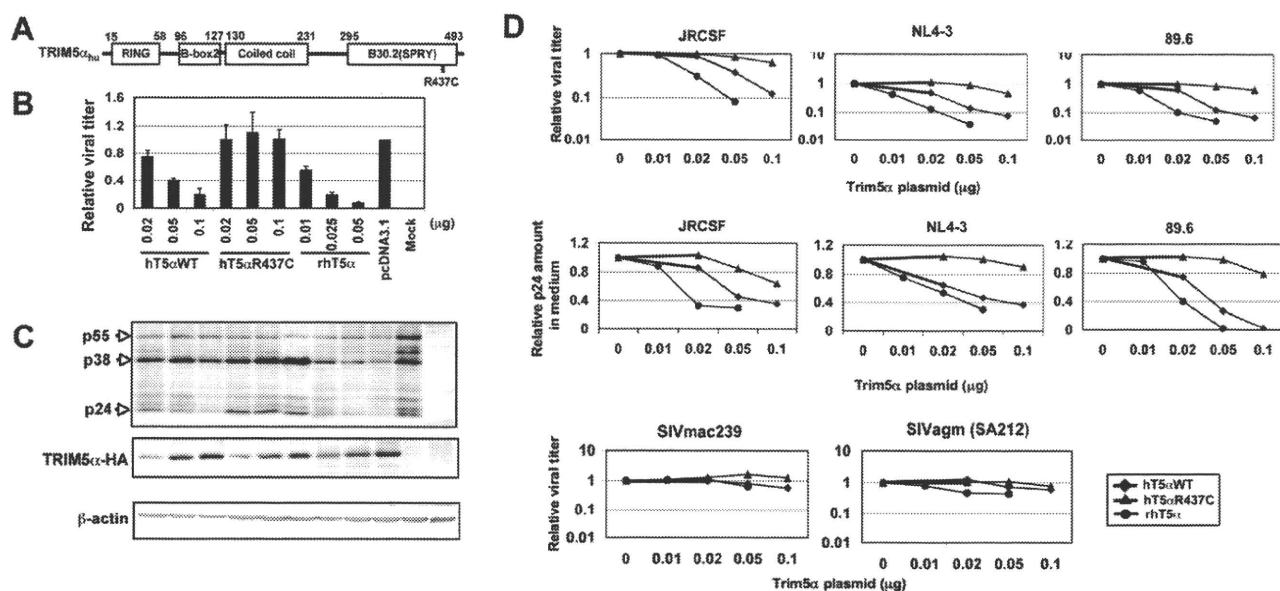


Fig. 1. Effect of overexpressed TRIM5 $\alpha_{hu}$  on HIV-1 production. (A) A schematic presentation of TRIM5 $\alpha_{hu}$  protein with the domains labeled and domain boundaries numbered according to the amino acid residue. (B) 293T cells ( $2 \times 10^5$ ) were transfected with 0.01  $\mu$ g of pNL $\Delta$ polEGFP together with various amounts of TRIM5 $\alpha_{hu}$ -HA (hT5 $\alpha$ WT or R437C) and TRIM5 $\alpha_{rh}$ -HA expression plasmid (rhT5 $\alpha$ ). Note that we used half amount of pRhT5 $\alpha$  plasmid for transfection since we found half amount pRhT5 $\alpha$  expressed an equal amount of TRIM5 $\alpha$ -HA protein compared to pHuT5 $\alpha$ WT and pHuT5 $\alpha$ R437C. pCDM $\beta$ -gal (0.01  $\mu$ g) was also transfected as a control of transfection efficiency. The amount of released p24 in culture supernatant and  $\beta$ -gal activity in the cell lysate from pcDNA3.1-transfected cells was 38 ng/ml and  $8 \times 10^{-1}$  unit, respectively. The ratio of p24 to  $\beta$ -gal activity was set as 1. (C) Lysates from 293T cells expressing the HA-tagged TRIM5 $\alpha$  proteins were subjected to SDS-PAGE, and the expression of HIV-1 Gag proteins and TRIM5 $\alpha$  was detected by immunoblotting. The order of the samples applied is the same as B. The results of a typical experiment are shown. Similar results were obtained in four independent experiments. (D) 293T cells were transfected with pYK-JRCSF, pNL4-3, p89.6, pSIVmac239 or pSA212 together with various amounts of TRIM5 $\alpha$  expression plasmids as in (B). After 2 days, the amount of released HIV-1 p24 in culture supernatant was measured by ELISA. The progeny viruses produced were infected to TZM-bl cells, and luciferase activity induced in the TZM-bl cells was evaluated to titrate the infectious viruses. Both luciferase activity and p24 amount were divided by  $\beta$ -gal activity in the 293T cell lysates to calculate relative viral titer and relative p24 amounts. The p24 concentration in the culture medium of pYK-JRCSF, pNL4-3, or p89.6-transfected cells that did not receive TRIM5 $\alpha$  expression plasmid was 193.2 ng/ml, 102.7 ng/ml or 10.16 ng/ml, respectively. The luciferase activity in the TZM-bl cells infected with the corresponding progeny viruses was  $8.12 \times 10^5$ ,  $3.56 \times 10^5$  or  $2.03 \times 10^4$  relative light unit (RLU), respectively. The progeny viruses produced from 293T cells transfected with pSIVmac239 and pSA212 induced  $9.62 \times 10^3$  RLU, and  $1.3 \times 10^3$  RLU, respectively. The data represent a typical result of 2 independent experiments.

more potent as an inhibitor than TRIM5 $\alpha_{hu}$  wild type (Fig. 1B). In parallel, intracellular expression of p24 was reduced as levels of pHuT5 $\alpha$ WT and pRhT5 $\alpha$  increased, but was unaltered in cells transfected with pHuT5 $\alpha$ R437C (Fig. 1C). Since all TRIM5 $\alpha$  proteins were expressed similarly at protein level in the transfected cells (Fig. 1C), these results suggest that TRIM5 $\alpha_{hu}$  possesses the ability to restrict HIV-1 replication at late stage in its life cycle. Note that we used a half amount of pRhT5 $\alpha$  plasmid for transfection since we found a half amount pRhT5 $\alpha$  expressed an equal amount of TRIM5 $\alpha$ -HA protein in 293T cells compared to pHuT5 $\alpha$ WT and pHuT5 $\alpha$ R437C. Since the vector for expression of TRIM5 $\alpha_{hu}$  and TRIM5 $\alpha_{rh}$  are the same, the difference of the expression level of TRIM5 $\alpha$  was not due to the difference of the promoter. Probably, TRIM5 $\alpha_{rh}$  is more stable than TRIM5 $\alpha_{hu}$  in 293T cells. To further confirm that TRIM5 $\alpha_{hu}$  has restriction effect on HIV-1 production, we transfected 293T cells with infectious HIV-1 or SIV molecular clones together with a plasmid encoding various TRIM5 $\alpha$ . We measured the p24 concentration in culture medium and also evaluated the viral titers by infection of progeny viruses to the TZM-bl indicator cells. As shown in Fig. 1D, TRIM5 $\alpha_{hu}$  as well as TRIM5 $\alpha_{rh}$  efficiently block the progeny virus production of

JRCSF, NL4-3 and 89.6 in a dose dependent manner. In contrast, TRIM5 $\alpha_{hu}$  R437C slightly limited the progeny viral production only when the highest amount of pHuT5 $\alpha$ R437C was co-transfected. Meanwhile, neither TRIM5 $\alpha_{hu}$ , TRIM5 $\alpha_{rh}$  nor TRIM5 $\alpha_{hu}$  R437C had significant effect on production of SIVmac239 and SIVagm (SA212) (Fig. 1D, lower panel). These observations clearly show the inhibitory effect of TRIM5 $\alpha_{hu}$  on HIV-1 production.

### 3.2. Incorporation of TRIM5 $\alpha$ into HIV-1 virions

Previous studies have shown that TRIM5 $\alpha_{rh}$  associates with HIV-1 precursor Gag and is incorporated into HIV-1 virions [17]. Since our ELISA results indicated that p24 levels were significantly lower in the medium of TRIM5 $\alpha_{rh}$ - as well as wild type TRIM5 $\alpha_{hu}$ -transfected cells (see Fig. 1B), we analyzed the formation of virion like particles (VLPs) in the culture media and the incorporation of TRIM5 $\alpha$ . As shown in Fig. 2, p24 levels in the VLP fraction were decreased in a dose dependent manner by TRIM5 $\alpha_{hu}$  and TRIM5 $\alpha_{rh}$  but not by TRIM5 $\alpha_{hu}$  R437C, supporting the inhibitory effect of TRIM5 $\alpha_{hu}$  on virus production and consistent with the results of the p24 ELISA (See Fig. 1B). However, while TRIM5 $\alpha_{rh}$  was

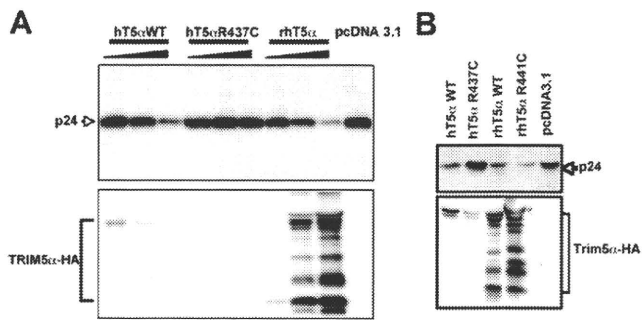


Fig. 2. Incorporation of TRIM5 $\alpha$  into HIV-1 virion. Culture supernatants of the 293T cells co-transfected with pNL $\Delta$ polEGFP and various TRIM5 $\alpha$  plasmids were harvested and passed through 0.45  $\mu$ m filter followed by ultracentrifugation through 20% sucrose layer. The VLP fractions prepared from 1 ml out of total 2 ml culture medium were applied to immunoblotting to detect the HIV-1 Gag proteins and incorporated TRIM5 $\alpha$ . (A) pNL $\Delta$ polEGFP (0.01  $\mu$ g) was transfected together with increasing amounts of TRIM5 $\alpha_{hu}$ -HA (hT5 $\alpha$ WT or R437C) and TRIM5 $\alpha_{rh}$ -HA expression plasmid (rhT5 $\alpha$ ) as indicated in Fig. 1B. (B) pNL $\Delta$ polEGFP (0.01  $\mu$ g) was transfected along with 0.1  $\mu$ g of TRIM5 $\alpha_{hu}$ -HA (hT5 $\alpha$ WT or R437C) or 0.05  $\mu$ g TRIM5 $\alpha_{rh}$ -HA expression plasmid (rhT5 $\alpha$ WT or R441C).

readily detected in VLP lysates and was inversely correlated with P24 levels, less amount of wild type TRIM5 $\alpha_{hu}$  was detected in VLP fractions, and the mutant TRIM5 $\alpha_{hu}$  was only marginally existent or even absent (Fig. 2A). These results suggest TRIM5 $\alpha_{hu}$  has weaker affinity for Gag than TRIM5 $\alpha_{rh}$ , which is consistent with our finding that TRIM5 $\alpha_{rh}$  inhibited HIV-1 more strongly than wild type TRIM5 $\alpha_{hu}$  (Fig. 1B).

### 3.3. The corresponding mutation in TRIM5 $\alpha_{rh}$ has no effect on its late restriction activity

An important question is that whether this arginine is also required for rhesus TRIM5 $\alpha$ , since it had been reported that SPRY domain of TRIM5 $\alpha_{rh}$  is dispensable to inhibit HIV-1 production [17,21]. We mutated arginine residue to cysteine at 441a.a. of TRIM5 $\alpha_{rh}$ , which corresponds 437a.a. of TRIM5 $\alpha_{hu}$ , and selected a clone that can express the HA-tagged mutant TRIM5 $\alpha_{rh}$  protein at the same level as the wild type. We co-transfected the TRIM5 $\alpha_{rh}$  mutant with pNL $\Delta$ polEGFP to 293T cells, and then investigated the effect of the mutant on HIV-1 production and encapsidation into virions. As shown in Fig. 2B, R441C TRIM5 $\alpha_{rh}$  mutant restricted HIV-1 production as severely as the wild type, and similar amounts of both wild type and mutant TRIM5 $\alpha_{rh}$  proteins were incorporated into virions. These results are in consistence with Sakuma's report [17,21].

### 3.4. Knockdown of endogenous TRIM5 $\alpha$ restores HIV-1 production

To examine the inhibitory effect of TRIM5 $\alpha_{hu}$  under physiological conditions, siRNA was used to suppress TRIM5 $\alpha_{hu}$  expression. Human HT1080 or 293T cells were co-transfected with pNL $\Delta$ polEGFP and control siRNA or siRNA

against TRIM5 $\alpha_{hu}$ . As shown in Fig. 3A, p24 production was enhanced roughly 3 fold upon knockdown of TRIM5 $\alpha_{hu}$  in HT1080 cells but was not altered in 293T cells in which TRIM5 $\alpha_{hu}$  was expressed at low levels. In parallel, the amount of cellular TRIM5 $\alpha_{hu}$  mRNA was markedly reduced in HT1080 cells, but much less in 293T cells (Fig. 3A left panel). It was noted that 293T cells produced over 170 times more p24 (58.68 ng/ml and 0.34 ng/ml, respectively) and expressed 110 times higher  $\beta$ -galactosidase activities (data not shown) than HT1080 cells, probably because of the better efficiency of transfection to 293T cells.

Next, we examined the effect of TRIM5 $\alpha_{hu}$  knockdown on HIV-1 production in HIV-1 host cells. As a first step, we examined the level of expression of TRIM5 $\alpha_{hu}$  in several T and macrophage cell lines (such as Jurkat, Molt4, MT-4, U937, and HL60) by quantitative RT-PCR and found that Jurkat E6-1 cells express the highest level of TRIM5 $\alpha_{hu}$  mRNA (Supplemental Information Fig. 1). We then transfected pNL $\Delta$ polEGFP to these T cell lines by electroporation and evaluated the p24 production in the culture media. While JurkatE6-1, Molt4, and MT-4 showed similar transfection efficiency, MT-4 produced highest level of p24 (2.34 ng/ml) compared with Molt4 and JurkatE6-1 (250 pg/ml and 114 pg/ml, respectively). This is reverse relation to the levels of Trim5 $\alpha_{hu}$  mRNA (Supplemental Information Fig. 2). Next we examined the effect of TRIM5 $\alpha$  knockdown on HIV-1 production in JurkatE6-1 cells. siRNA against TRIM5 $\alpha_{hu}$  together with pNL $\Delta$ polEGFP were electroporated into the cells. Forty-eight hours later, the abundance of TRIM5 $\alpha_{hu}$  mRNA was reduced to 35%, and concomitantly the amount of p24 Gag in the culture media was increased about 2.5 times compared to control siRNA (Fig. 3B). These results demonstrate that endogenous TRIM5 $\alpha_{hu}$  is able to restrict HIV-1 progeny production.

### 3.5. Effect of the TRIM5 $\alpha_{hu}$ R437C mutant on HIV-1 entry

The mutation R437C in TRIM5 $\alpha_{hu}$  is located in the SPRY domain, in which alteration of a single amino acid has been reported to modulate TRIM5 $\alpha$  restriction potency against HIV-1 infection at an early stage [35]. Therefore, we examined whether there was any difference between wild type TRIM5 $\alpha_{hu}$  and the R437C mutant in restricting HIV-1 infection early in infection. At first we examined the effects of various Trim5 $\alpha$ s, which were transiently expressed in 293T cells by transfection of pHuT5 $\alpha$ WT, pRhT5 $\alpha$ , and pHuT5 $\alpha$ R437C, on the efficiency of infection of HIV-1-Venus that had been pseudotyped with VSV-G glycoprotein. The cells expressing TRIM5 $\alpha_{hu}$ WT and TRIM5 $\alpha_{hu}$  R437C showed slightly decreased rate of HIV-1-Venus infection compared with the control vector pcDNA3.1-transfected cells, whereas TRIM5 $\alpha_{rh}$ -expressing cells were markedly resistant (Fig. 4A). To confirm this result, using a retrovirus vector we established stable HeLa cells that express TRIM5 $\alpha_{hu}$ WT, TRIM5 $\alpha_{hu}$  R437C, and TRIM5 $\alpha_{agm}$ . The cells were then infected with pseudotyped HIV-1-Venus as above. Similarly, TRIM5 $\alpha_{agm}$ -



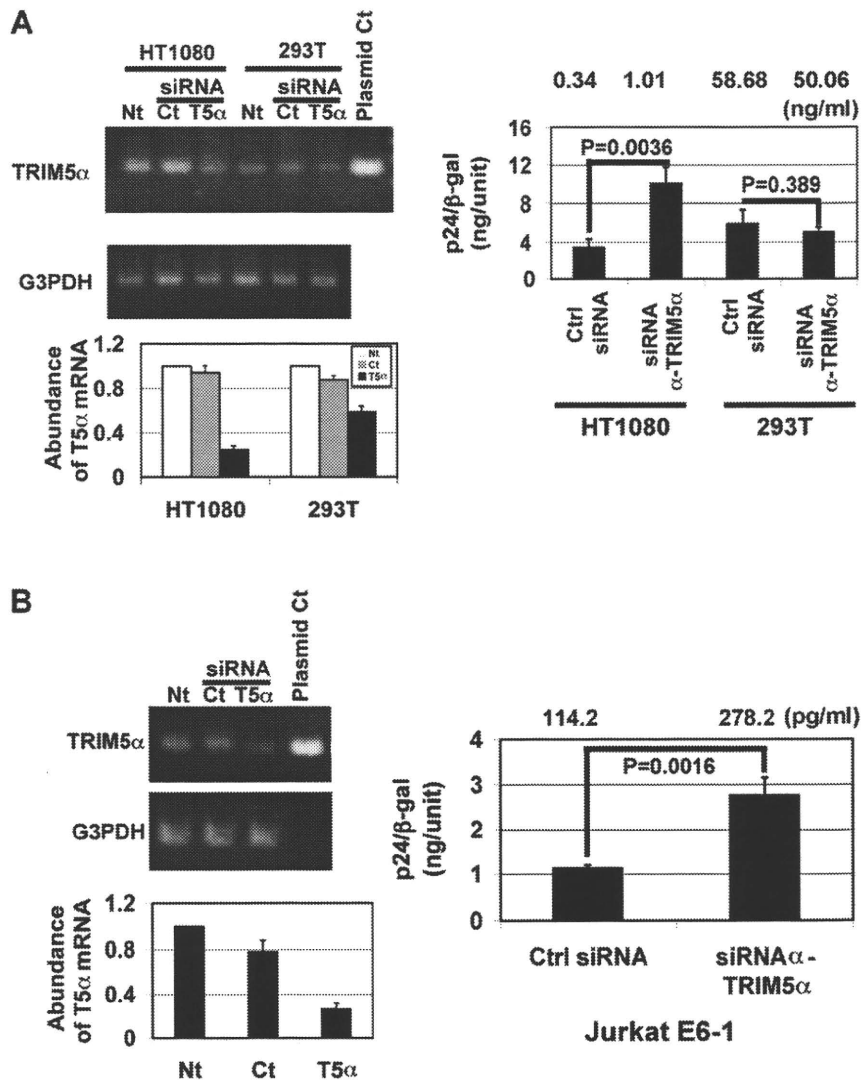


Fig. 3. Effect of knockdown of TRIM5 $\alpha$  in human cells on HIV-1 production. (A) HT1080 or 293T cells were co-transfected with pNL $\Delta$ poEGFP and control siRNA or siRNA against Trim5 $\alpha$ <sub>hu</sub>. (B) Jurkat E6-1 cells were electroporated with the plasmid and siRNAs described above by nucleofection. pCDM- $\beta$ -gal was also included in both A and B to monitor the transfection efficiency. After 2 days, p24 levels in the supernatants and  $\beta$ -gal activity in the cell lysates were measured. The relative p24 production was calculated by dividing p24 amount by  $\beta$ -gal activity (right panel of A and B). The p24 levels in the culture media are indicated on the top of right panels of A and B. The level of TRIM5 $\alpha$  expression was examined by usual and quantitative RT-PCR. Cells that were not subjected to any treatment (Nt) were used as blank controls. The pictures of RT-PCR in the left panels represent a typical one of 3 independent experiments. The results of quantitative PCR represent the mean  $\pm$  S.D. of triplicate samples.

expressing cells were markedly resistant to infection, By contrast, the marginal inhibitory effect on HIV-1 infection was observed for the cells expressing TRIM5 $\alpha$ <sub>hu</sub>WT and TRIM5 $\alpha$ <sub>hu</sub> R437C (Fig. 4C). Since all TRIM5 $\alpha$ s were identically expressed (Fig. 4B and D), the difference in HIV-1 infection efficiency was not due to differences in TRIM5 $\alpha$  levels. These results suggest that the mutation at residue 437 of TRIM5 $\alpha$ <sub>hu</sub> has subtle effect on HIV-1 infection at the post-entry stage.

### 3.6. Effect of TRIM5 $\alpha$ <sub>hu</sub> R437C on N- and B-MLV infection

TRIM5 $\alpha$ <sub>hu</sub> has been shown to restrict N-tropic but not B-tropic MLV infection [10]. Since the coiled-coil and the

SPRY domains have been reported to be involved in this processes, we investigated whether the amino acid substitution at residue 437 in the SPRY domain alters the ability of TRIM5 $\alpha$ <sub>hu</sub> to inhibit N-tropic MLV infection. Wild type and mutant TRIM5 $\alpha$  expressing 293T cells were established and infected with VSV-G-pseudotyped N-tropic and B-tropic MLV at various doses. In comparison with 293T cells transduced with the empty MX-puro vector, cells expressing wild type TRIM5 $\alpha$ <sub>hu</sub> or TRIM5 $\alpha$ <sub>agm</sub> were markedly resistant to infection with N-MLV but susceptible to B-tropic MLV, consistent with previous reports [36] (Fig. 5A). N-tropic MLV was infected to the R437C mutant expressing cells as efficiently as cells transduced with the empty MX-puro vector. Cells expressing TRIM5 $\alpha$ <sub>rh</sub> were susceptible as well,